Use of thermal modeling to assess the tectono-metamorphic history of the Lugo and Sanabria gneiss domes, Northwest Iberia

JAMES E. ALCOCK[1], JOSÉ R. MARTÍNEZ CATALÁN[2], RICARDO ARENAS[3] and ALEJANDRO DÍEZ MONTES[4]

Keywords. – Gneiss domes, Thermal modeling, Variscan orogeny, Northwest Iberia

Abstract. – The Lugo and Sanabria domes in Northwest Iberia have well constrained metamorphic and structural histories. Both occur in the Iberian autochthon and resulted from late-Variscan extensional collapse following crustal thickening related to the Variscan collision. The two domes developed beneath large thrust sheets, are cored by sillimanite-orthoclase anatectic gneiss, preserve evidence of a steep thermal gradient (≈ 1 °C MPa^{-1}), and exhibit a distinct decrease in metamorphic grade to the east in the direction of nappe movement. Geochronological evidence indicates that the lower crust melted within $\approx$ 30 Ma of initial crustal thickening and that dome formation occurred within 50 Ma.

The histories of the two domes are considered as the basis for one-dimensional finite-difference models of thermal response to changes in crustal thickness. Results from thermal models suggest that thickening was limited to the crust, provide a numeric explanation for timing and nature of granite magmatism, and indicate that high-temperature metamorphism and crustal anatexis may result directly from thermal relaxation, eliminating the need for significant mantle thermal contribution. Also, the models show that small differences in thickness of large, wedge-shaped thrust sheets can explain distinct P-T paths experienced by different limbs of the domes.

Emploi des modèles thermiques pour évaluer l'histoire tectono-métamorphique des dômes gneissiques de Lugo et Sanabria, Nord-Ouest de l'Ibérie

Mots-clés. – Dômes gneissiques, Modèles thermiques, Orogenèse varisque, Nord-Ouest de l'Ibérie

Résumé. – L'évolution métamorphique et structurale des dômes de Lugo et Sanabria, dans le Nord-Ouest de l'Ibérie, sont bien connues. Les deux se sont formées dans l'autochtone du Massif ibérique en réponse à l'effondrement gravitaire de la chaîne varisque. Les deux dômes se sont développés au-dessous de grandes nappes de chevauchement, leur coeur étant occupé par des gneiss anatectiques à sillimanite-orthose, préservant des évidences d'un gradient métamorphique assez fort (≈ 1 °C MPa^{-1}) et sont caractérisés par une diminution des conditions métamorphiques vers l'est, dans la direction du mouvement des nappes. Les données géochronologiques indiquent que la fusion partielle commença 30 millions d'années et la formation des dômes 50 millions d'années après le début de l'épaississement crustal.

Les histoires P-T des deux dômes sont choisies pour étudier la réponse thermique aux variations d'épaisseur crustale en utilisant la modélisation thermique par la méthode des différences finies en une dimension. Les résultats indiquent que l'épaississement a été limité à la croûte continentale, fournissant une explication numérique pour l'âge et la nature du magmatisme granitique et suggérant que le métamorphisme de haute température et l'anatexie crustale peuvent être la conséquence de la relaxation thermique, sans nécessairement invoquer une contribution significative d'une source mantélique. De plus, les modèles montrent que de petites différences dans l'épaisseur des nappes de chevauchement expliquent les différences de trajectoires P-T suivies par les deux flancs des dômes.

INTRODUCTION

England and Thompson [1984], Thompson and England [1984], and Peacock [1989] showed how to model the pressure-temperature-time (P-T-t) paths of regional metamorphism in regions of thickened continental crust. Their models place the physical conditions undergone by rocks initially at different depths in a temporal frame, permit a better understanding of the orogenic processes involved, and explain very elegantly the succession of metamorphic facies and granite generation [England and Thompson, 1986]. Further development of P-T-t modeling covers special cases in orogenic belts [Davy and Gillet, 1986; Thompson and Ridley, 1987], and the subduction and obduction of oceanic lithosphere [Peacock, 1990, 1991; Jamieson, 1986].

The results of general thermal modeling have been widely applied in regional and local studies to interpret tectono-metamorphic histories deduced from mineral assemblages of

1. Department of Geosciences, Abington College, Penn State University, Abington, PA 19001, USA, e-mail: jea4@psu.edu
2. Departamento de Geología, Universidad de Salamanca, 37008 Salamanca, Spain, e-mail: jrmc@usal.es
3. Departamento de Petrología y Geoquímica e Instituto de Geología Económica [CSIC], Universidad Complutense, 28040 Madrid, Spain, e-mail: rarenas@geo.ucm.es
4. Instituto Geológico y Minero de España, Azafranal 48, 37001 Salamanca, Spain, e-mail: al.diez@igme.es
Manuscrit déposé le 22 janvier 2008 ; accepté après révision le 23 mai 2008

metamorphic rocks and their chemical equilibrium [Spear, 1989]. In most instances, the geologists built P-T paths (or P-T-t, P-T-d, P-T-t-d, where t stands for time and d for deformation) from field and laboratory data, and use them to infer aspects of the processes undergone by metamorphic rocks, such as geotectonic settings, amount of thickening and thinning, burial and exhumation rates, and the importance of tectonic versus erosional denudation. Such an approach has been used in Northwest Iberia for the interpretation of exotic, allochthonous terranes [Gil Ibarguchi and Arenas, 1990; Arenas, 1991; Arenas *et al.*, 1995, 1997; Martínez Catalán *et al.*, 1996; Abati *et al.*, 2003] and also to decipher the evolution of the Iberian autochthon at extensional gneiss domes [Escuder Viruete *et al.*, 1994, 1997, 2000; Arenas and Martínez Catalán, 2003].

Here, we propose a quite different use of thermal modeling: assessing what is known about the evolution of particular structures or regions. Comparing the available structural and petrologic data with model results may help to constrain the deduced tectono-metamorphic history either showing that it is reasonable or by identifying potential inconsistencies and errors. Furthermore, comparison between field results and models may provide hints to a wider understanding of the orogenic process, in particular, concerning the involvement of the deep parts of the crust and lithosphere that cannot be directly observed.

Gneiss domes are common structures in orogenic belts. They are formed during the late orogenic stages associated with extensional processes, and the involved rocks have registered the whole thermobaric history of the belt at a wide range of depths. Thermomechanical modeling has been applied to gneiss domes of different types to understand their evolution by Burg *et al.* [2004], Fayon *et al.* [2004], Gerya *et al.* [2004] and Tirel *et al.* [2004].

This work carries out numerical models on the thermobaric evolution of two such structures, the Lugo and Sanabria gneiss domes, and compares our geological knowledge with the model results obtained. Both structures are geologically well known and representative of the Variscan thickening and subsequent extension by gravitational collapse of the orogen. The initial and boundary conditions are derived from the regional geological background, which includes the geometry and nature of the main tectonic, metamorphic and magmatic events and their approximate age. For the physical parameters of rocks, standard values given in the geological literature are used, adapted to the particular case. Available estimates of the P-T paths deduced from the mineral associations are a very important constraint for model evaluation, but do not form part of the boundary conditions. Instead, the known P-T evolution is the reference to which the results of thermal modeling are compared, providing a test for the validity of the assumptions concerning the orogenic evolution and/or the physical parameters and the numerical models. Published isotopic ages of granitoids are also used to test the accuracy of the models.

Modeling is used here to shed light on regional aspects of the orogenic evolution such as the age of the main deformation events, the amount of crustal thickening and thinning undergone, the strain rates, and to evaluate existing $P - T \pm t \pm d$ paths inferred from structure, geochronology and mineral petrogenesis. Model results partly conform to prior inferences; however, there are a few areas in which the results require re-examination of prior interpretations, such as mantle delamination occurring late in the orogenic cycle, and the inferred isobaric P-T paths of rocks in the footwall to major thrust sheets. Model data also suggest that thickening of the lithosphere was limited to the crust, a result that could not be directly inferred from existing geological data.

GEOLOGICAL SETTING

The Northwest Iberian Variscan basement consists of low- to high-grade metamorphic rocks and granitoids. Internal areas occur in the west or southwest, whereas the external zones crop out to the northeast. A distinction can be established between the Iberian autochthon and the allochthonous complexes (fig. 1), both being separated by the lower allochthon, a thrust sheet, several kilometres thick. Recent reviews on the evolution of Northwest Iberia are presented in Arenas *et al.* [2007] and Martínez Catalán *et al.* [2007].

The autochthon developed in a marginal part of northern Gondwana characterized by Archean and Paleoproterozoic basement. It underwent intensive Cadomian reworking during Neoproterozoic arc-continent collision [Montero *et al.*, 2007], and subsequent Cambro-Ordovician rifting related to peri-Gondwanan terrane dispersion. Both events produced abundant granitoids and felsic volcanics, presently transformed into orthogneisses. The succession includes a thick Neoproterozoic terrigenous sequence (Vilalba Series), a complete and thick Cambrian to Early Devonian shallow-water marine sequence, and a few synorogenic Carboniferous deposits. Slates and schists are the most common rocks, but sandstones, quartzites and carbonates are also abundant in the Paleozoic sequence, which is typical of a passive continental margin. The most continuous Paleozoic quartzite and carbonate formations have been drawn in the cross-sections of figure 2 to show the structure. Also important is an Early Ordovician volcanogenic unit several kilometers thick known as the Ollo de Sapo Fm, of rhyolitic and dacitic composition. Granitic orthogneisses of roughly the same age and geochemically related were intruded in the underlying successions [Díez Montes, 2007].

The lower allochthon (fig. 1) consists of Early Ordovician to Devonian metasediments, volcanic, and plutonic rocks, which can be correlated to those of the autochthon, from which they are separated by a large, low-dipping thrust fault [Farias *et al.*, 1987]. The allochthonous complexes are the remnant of a thick nappe pile preserved in the core of late Variscan synforms. They consist of a stack of units separated by thrusts faults and extensional detachments, which represent accreted, exotic terranes. These include pieces of rifted continental margins, volcanic arcs and oceanic lithosphere, many of them affected by subduction-related high-pressure metamorphism [Arenas *et al.*, 2007; Martínez Catalán *et al.*, 2007, and references therein].

The Lugo and Sanabria domes [Martínez *et al.*, 1988] form part of the autochthon, but their metamorphic and structural evolution was influenced by the emplacement of the allochthonous complexes. The evolution of the latter is too complex and beyond the scope to be dealt with here, but that of the domes is important for the models, and is described in the next sections.

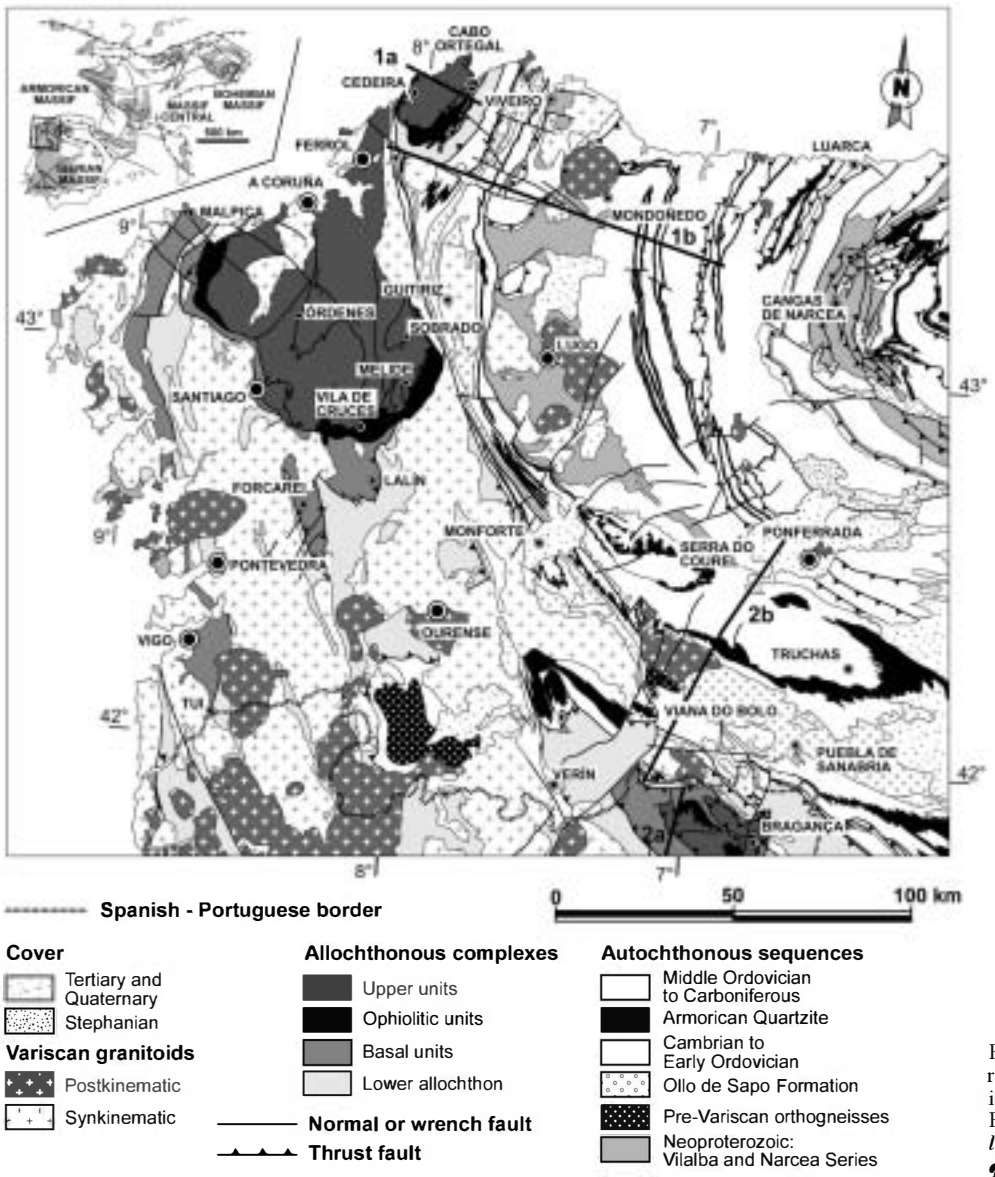

FIG. 1. – Geologic sketch of Northwest Iberia. The location of cross sections in figure 2 is indicated.
FIG. 1. – *Carte géologique du Nord-Ouest de l'Ibérie avec indication des coupes géologiques de la figure 2.*

STRUCTURE AND EVOLUTION OF THE LUGO AND SANABRIA DOMES

The Lugo dome [Capdevila, 1969] is a wide N-S antiformal structure, 140 km long and 35 km wide structure going from Viveiro, on the Cantabrian coast, to the Serra do Courel (fig. 1). Its core is occupied by the deep parts of the Mondoñedo nappe [Matte, 1968] and its relative autochthon. The nappe is a set of kilometric-scale recumbent folds floored by a thrust fault [Bastida *et al.*, 1986], below which the autochthon crops out in the Xistral tectonic window (fig. 2). The Sanabria dome [Díez Montes, 2007] is also an open antiform, 50 km long and 20 km wide, elongated in the NW-SE direction, and situated to the south of the Lugo dome, between Viana do Bolo and Sanabria (fig. 1). Its core is occupied by the Ollo de Sapo anticlinorium (fig. 2), characterized by relatively small recumbent folds, and where no thrust faults have been identified, although the Mondoñedo nappe crops out to the northeast and its basal thrust probably continues down below the dome.

The two antiforms are characterized by high-temperature Variscan metamorphism, reaching the sillimanite-orthoclase zone, and by a pervasive schistosity related to extensional tectonics. Partial melting is evident in migmatites developed at their cores, and in the voluminous Variscan granitoids intruded. Both antiforms are flanked by synforms. To the east, the Bretoña and Truchas synforms are very open structures cored by low-grade Paleozoic metasediments. To the west, two large normal faults, the Viveiro and Chandoiro faults (fig. 2) separate the antiforms from two open synforms that host the remnants of the allochthonous nappe pile forming the complexes of Cabo Ortegal and Bragança (figs. 1, 2).

On kinematic grounds, the Lugo and Sanabria antiforms do not seem to have developed in the footwall to extensional detachments by elastic rebound of the lithosphere. For the Lugo antiform to be interpreted in that way, the lower extensional shear zone and detachment should have a top-to-west kinematics, whereas it is just the opposite (fig. 2). For the Sanabria antiform, the stretching lineation

and shear sense associated with exhumation is nearly parallel to its axis, instead of being perpendicular. Both antiforms are interpreted as extensional gneiss domes in the sense of Burg *et al.* [1994] and Tirel *et al.* [2004], as they have granitic and migmatitic cores developed after Variscan crustal thickening, a strong subhorizontal fabric developed during exhumation, and are bounded by extensional detachments and normal faults. Their structural evolution includes shortening and crustal thickening, related to plate convergence, as well as extension and crustal thinning linked to gravitational collapse of the weakened orogenic crust. Several generations of structures permit the individualization of three contractional (C1, C2 and C3) and two extensional (E1 and E2) deformation events, although most of them are diachronous and may overlap in time. These structures and events are described briefly here, whereas more detailed descriptions are available in Bastida *et al.* [1986], Arenas and Martínez Catalán [2003], Martínez Catalán *et al.* [2003, 2004], and Díez Montes [2007]. Published geophysical data and interpretations include seismic profiling [Córdoba *et al.*, 1987; Ayarza *et al.*, 1998], and gravity and magnetic modeling [Ayarza and Martínez Catalán, 2007].

Recumbent folding (C1)

The first deformation event produced a regular train of folds, inclined to recumbent, with northeast vergence. Very large folds occur in the Mondoñedo nappe (fig. 2), where the largest overturned limb reaches 15-30 km due to post-folding horizontal shearing related in part to thrusting and in part to late orogenic extension. To the west and south, recumbent folds are common in low-grade areas, but they are smaller, their reverse limbs rarely attaining 5 km. A low-grade slaty cleavage or foliation (S_1) developed pervasively in the slates and in the Ollo de Sapo Fm. The associated stretching lineation, with along-dip attitude, indicates that the deformational flow was perpendicular to the orogenic trend, so that significant strike-slip components seem not to be associated to early folding.

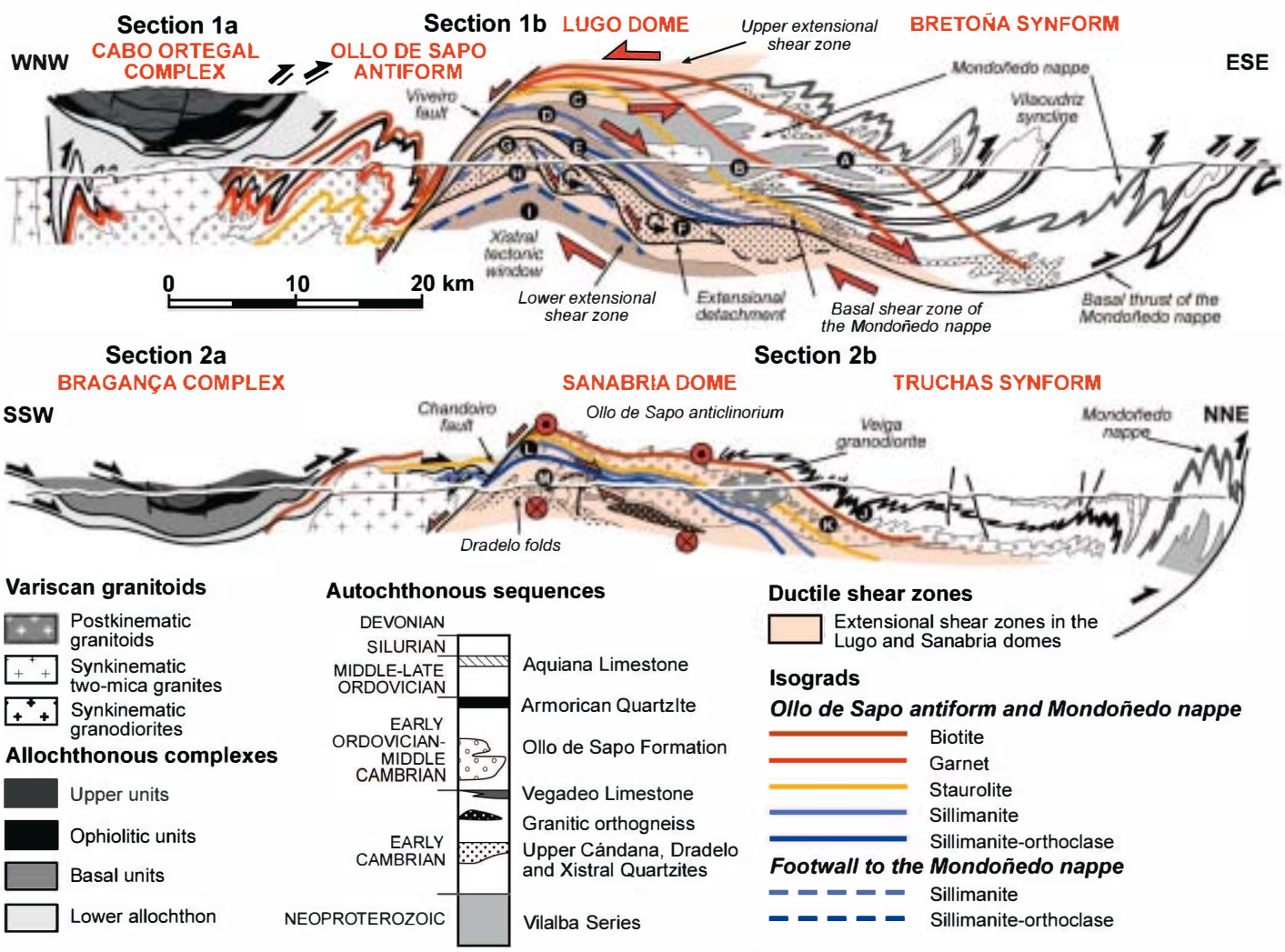

FIG. 2. – Geologic sections across the Lugo and Sanabria domes and adjacent synforms. Capitals in black circles mark the location of P-T paths of figure 3. Based on Marcos *et al.* [1984, 2002 ; section 1a], Martínez Catalán *et al.* [2003, 2004 ; section 1b] and Díez Montes [2007 ; section 2]. The circle and dot symbol indicates a sense of movement to the reader in the Sanabria shear zone. See figure 1 for location of sections.

FIG. 2. – *Coupes géologiques au travers des dômes de Lugo et Sanabria et des synformes adjacents. Les majuscules dans un cercle noir indiquent la localisation des trajectoires P-T dans la figure 3. D'après Marcos* et al. *[1984, 2002 ; coupe 1a], Martínez Catalán* et al. *[2003, 2004 ; coupe 1b] et Díez Montes [2007 ; coupe 2]. Le symbole avec un cercle et un point indique un sens de cisaillement vers le lecteur dans la zone de cisaillement de Sanabria. Voir figure 1 pour la localisation des coupes.*

The folds are well developed in the Armorican Quartzite, a 200-400 m thick competent layer that controlled the buckling processes during folding. These are commonly of the flattened parallel type [Ramsay, 1967]. An area where C1 folds crop out exceptionally well and have been little affected by subsequent deformations was selected in the southern limb of the Truchas synform to calculate the horizontal stretch associated to folding. Several orthogonal sections, ranging from individual metric folds to panoramic views, were analyzed first by estimating the superimposed flattening, then removing it, and finally measuring the length of the beds and comparing it with the final horizontal lengths. To estimate the superimposed flattening, we used dip isogons [Ramsay, 1967; Hudleston, 1973; Ramsay and Huber, 1987] and a modified version of the computer program Isogons [Vacas Peña, 2001].

The value obtained for the horizontal stretch, which is the ratio of deformed to undeformed lengths [Means, 1976] varies between 0.8 and 0.5, with a mean of 0.67. This includes shortening by buckling, plus superimposed flattening, but not initial layer-parallel shortening, which is difficult to estimate. These values have been obtained assuming that deformation was of the plane strain type, that is, no changes in the surface of the orthogonal sections occurred. This implies no significant volume change, and no elongation in the direction normal to the section. If these assumptions are generalized to the whole crust, a stretch of 0.67 is equivalent to a shortening of 33%, and would result in a crustal thickening factor of 1.5 or 150%.

For the Mondoñedo nappe, fold analyses were carried out by Bastida [1981] and Martínez Catalán [1985] in Cambrian and Ordovician quartzites. Shortening perpendicular to the axial surfaces vary between 37 and 59%, which, considering pure shear, implies thickening parallel to the axial surface between 158 and 243%. As the axial surface is inclined instead of vertical, these numbers do not translate directly into values for vertical thickening, but suggest that shortening was higher here than in the Truchas synform.

$^{40}Ar/^{39}Ar$ dating of regional cleavage (S_1) yielded 359 Ma to the south of Puebla de Sanabria and close to the allochthonous complex of Bragança, and 336 Ma to the east of the Mondoñedo nappe, indicating the diachronous character of deformation and its progradation from west to east, that is, toward the external zones of the belt [Dallmeyer *et al.*, 1997].

Thrusting (C2)

The second deformation is characterized by the movement of thrust sheets directed toward the external zones. Thrusts significant to our research are those associated to the emplacement of the allochthonous complexes, and the basal thrust of the Mondoñedo nappe.

The allochthonous complexes were first placed over the lower allochthon and in turn, it was thrust onto the autochthon carrying the allochthonous complexes piggyback and crosscutting the C1 folds in the footwall. In the Órdenes Complex, the largest and thickest of the allochthonous complexes (fig. 1), the cumulative thickness shown by the different units approaches 20 km including the lower allochthon [Martínez Catalán *et al.*, 2002]. Taking into account that erosion has occurred since its emplacement, the allochthonous sheet should have been more than 20 km thick. However, as the Órdenes Complex occupy a more internal position than the domes we have studied, and the allochthon was presumably wedge-shaped tapering to the E, we would consider 20 km as the maximum thickness of the allochthonous sheet above the domes in the numerical models.

Pressure estimations were made by Arenas [1988, 1991] based on the composition of phengites in Silurian metapelites underlying the Cabo Ortegal Complex. The dominant phengite generation yielded 400 °C and 0.25-0.3 GPa ($\approx$ 11 km), interpreted as conditions after C2. An old generation of phengites whose composition suggests conditions of 325 °C and 0.2 GPa (equivalent to 7.5 km), may well represent conditions after the C1 recumbent folding. The data imply that roughly 10-15 km of allochthon replaced 5-10 km of the footwall, loading the autochthon only with 5-10 km of new crust.

Thrusting of the Mondoñedo nappe followed the emplacement of the allochthonous complexes. Its basal thrust crosscut C1 recumbent folds in both the hanging wall and footwall units. A ductile shear zone 3 km thick occurs at the base of the Mondoñedo nappe (fig. 2), and has been related to nappe emplacement by Bastida *et al.* [1986], and Aller and Bastida [1993]. However, although a portion of shearing may be related to thrusting, a significant part of it seems actually linked to subsequent extension [Martínez Catalán *et al.*, 2004; Ayarza and Martínez Catalán, 2007].

From its presently preserved thickness (fig. 2), we infer that the Mondoñedo nappe was more than 10 km thick when emplaced. The pressure estimated at the top of its relative autochthon in the Xistral tectonic window, between 0.2 and 0.4 GPa [Arenas and Martínez Catalán, 2003], suggests a reduced thickness during the emplacement. But its basal rocks had previously reached 0.9 GPa, $\approx$ 35 km [Reche *et al.*, 1998], partly by the overburden of the allochthonous complexes. Consequently, the thrust sheet was considerably thinned by internal deformation and/or erosion prior to or during emplacement [Martínez Catalán *et al.*, 2003].

The timing of thrusting was bracketed by Dallmeyer *et al.* [1997; $^{40}Ar/^{39}Ar$ method] to be between 343 and 321 Ma. The older is the age of the thrust-related foliation in the lower allochthon, and the latter is the age of a thrust some 40 km to the east of the Mondoñedo nappe front. These ages show the diachronism and progradation of thrusting to the external zones. The Mondoñedo thrust is not dated but, given its intermediate position, an age of 330-325 Ma seems reasonable.

Extension and gravitational collapse (E1)

Following the emplacement of the allochthon and thrust imbrication of the autochthon, a pervasive subhorizontal tectonic foliation (S_2) developed in the middle and lower parts of the autochthonous section linked to extension, as indicated by the presence of two conjugate extensional shear zones affecting the Mondoñedo nappe and its autochthon (fig. 2). The crustal wedge between them escaped eastward, whereas the previous Barrovian metamorphic zones were thinned and the isograds approached each other in the upper shear zone.

Kinematic criteria demonstrate a non-coaxial component of deformation, and mostly indicate extension E-W, normal to the orogenic trend. In the autochthon, large blocks of thick and competent Xistral Quartzite were

rotated during extension by domino-style boudinage just below the Mondoñedo basal thrust (fig. 2). The base of the nappe was sheared with a top-to-the east sense of movement, deforming synkinematic granitoids and showing that the nappe and its footwall were strongly overprinted by the E1 extensional event.

In Sanabria, a broad shear zone developed structurally below the biotite isograd, with characteristics similar to the lower extensional shear zone of the Lugo dome. The stretching lineation and kinematic criteria indicate top-to-the southeast sense of shearing, which here is roughly parallel to the orogenic trend.

The cause of extension was probably heat accumulation due to crustal thickening, although advection by mantle-derived rocks [Galán *et al.*, 1996] might also have contributed. Heat lowered the viscosity of the middle and lower crust, caused partial melting, and facilitated viscous flow that accommodated extension of the whole crust, probably in response to gravitational forces [Martínez Catalán *et al.*, 2003, 2004].

The first extensional event has been dated in migmatites in the Sanabria dome at 311-314 Ma [U-Pb ages in monazites; Díez Montes, 2007]. In the Lugo dome, timing of E1 is constrained by age data of the Variscan granitoids, which will be described in a later section. Granite massifs deformed by the extensional shear zones range between 323 and 313 Ma, whereas undeformed, postkinematic massifs yield ages of 295-285 Ma [Fernández-Suárez *et al.*, 2000]. If the deformed granitoids were strictly synkinematic, their age is that of E1 extension. If they preceded extension, their dating provide a maximum age limit for E1, with a minimum age limit at 295 Ma in any case.

Comparable granitoids in the Sanabria dome are little deformed to undeformed by E1, but can be affected by C3 strike-slip shear zones [Vegas *et al.*, 2001]. The fact that synkinematic granitoids are often affected by subhorizontal foliations in the Lugo dome [Martínez Catalán, 1985; Bastida *et al.*, 1986; Aranguren and Tubía, 1992] suggests that E1 extension is younger there than in Sanabria. This would imply progradation of extension toward the external zones, which is congruent with the progradation to the east of contractional events C1 and C2 [Martínez Catalán *et al.*, 2007].

Late folding (C3)

The third contractional deformation is characterized by upright folding, closely related to the contemporaneous activity of subvertical shear zones with wrench, mostly dextral components [Iglesias Ponce de León and Choukroune, 1980; Martínez Catalán *et al.*, 2007].

Late C3 folds can be identified by their associated crenulation cleavage (S_3) and because they fold the metamorphic isograds. They are upright to vertical, well developed and tight in the Ollo de Sapo antiform, but in the core of the Sanabria dome, the C3 Dradelo folds are overturned and even recumbent, due to overprinting by the dome (fig. 2). In both cases, C3 folds overprint the extensional foliation (S_2). However, C3 folds are rare and open in the Lugo dome, which suggests that the main extension occurred here after the C3 event.

Probably, late folding did not induce significant crustal thickening, because it is associated with an horizontal stretching lineation and related to strike-slip movements. The fact that it occurred during the extensional collapse implies renewed shortening, probably related to oblique plate convergence. However, the crust was weak and did not allow contractional stresses to build up a new significant crustal root, so that shortening was mostly resolved by horizontal flow.

The age of late folding has been established at 314 ± 6 Ma by dating synkinematic granitoids [Capdevila and Vialette, 1970; Ries, 1979], and at 315 and 305 Ma by dating the motion of strike-slip shear zones [Regêncio Macedo, 1988; Valle Aguado *et al.*, 2005]. These ages partially overlap those of E1 extension, and suggest that C3 folding was an isochronous contractional event intercalated in a longer and diachronous episode of orogenic collapse and extension.

Late extension and doming (E2)

Late stages of collapse and extension are characterized by doming and the late development of the Viveiro and Chandoiro normal faults (fig. 2). We suggest that the domes were formed by lateral flow and ascent of ductile, low-density migmatitic gneisses, as proposed for this kind of structures by Block and Royden [1990], Tirel *et al.* [2004], and Whitney *et al.* [2004], but possibly coinciding with weakened areas subjected to renewed extension. The normal faults would represent the transition from ductile to brittle behaviour in the very late stages of extension.

E1 and E2 extensional events together were responsible for the return of the Variscan crust to a normal thickness. The difference in the maximum pressure registered by rocks cropping out in both sides of the Viveiro fault was estimated by Reche *et al.* [1998] using thermobarometry, to be 0.4-0.5 GPa, roughly equivalent to 15-19 km. This offset results from the combined effect of the two conjugate extensional shear zones joining each other close to the fault, and the fault itself. A throw of 5-6 km is more reasonable for the Viveiro fault alone [Martínez Catalán *et al.*, 2003], and a similar throw can be assumed for the Chandoiro fault [Díez Montes, 2007].

Timing of E2 is constrained by $^{40}Ar/^{39}Ar$ cooling ages around 300 Ma in the Lugo dome [Dallmeyer *et al.*, 1997], and by the Veiga granodiorite in Sanabria, dated at 286 ± 6 Ma [Ortega *et al.*, 2000], and deformed and cut by the Chandoiro fault [Román-Berdiel *et al.*, 1995], so dating latest stages of dome development.

METAMORPHIC EVOLUTION

Lugo dome

Metamorphism in the Lugo dome was first described by Capdevila [1969] as of intermediate-low pressure type. It was further studied by Reche *et al.* [1998], who carried out thermobaric calculations, and by Arenas and Martínez Catalán [2003], who traced P-T paths for the Mondoñedo nappe and its autochthon (fig. 3A) using mineral associations and the petrogenetic grid for pelites of Powell and Holland [1990].

In the Mondoñedo nappe, a classic Barrovian succession including the chlorite, biotite, almandine and staurolite zones point to an initial gradient of intermediate pressure. Kyanite occurs sparsely, and has been found as a relict phase in the sillimanite-orthoclase zone, in the sheared rocks close to the Viveiro fault and in a few points of the biotite zone. A later

low-pressure gradient is indicated by garnet and staurolite-bearing rocks entering into the sillimanite and andalusite fields. The P-T paths (fig. 3A, paths A to E) evolved along the intermediate pressure field during prograde metamorphism, related to crustal thickening (dashed, unconstrained part of paths A and B). Then, they show a strong decompression and enter into the low pressure field. Reche *et al.* [1998] describe kyanite developed after andalusite in Ordovician and Silurian metapelites surrounding the Viveiro fault, but this transformation was not included in the P-T paths of Arenas and Martínez Catalán [2003] shown in figure 3A.

For the relative autochthon of the nappe (grey arrows F to I, fig. 3A), the P-T paths were traced always in the low pressure field, because of the absence of kyanite, scarcity of garnet, and abundance of cordierite. The upper part of the footwall to the nappe was in the chlorite-biotite zone during thrusting, whereas deeper zones reached the staurolite zone, sometimes accompanied by garnet. Cordierite was also profusely developed in these rocks. Still deeper, the sillimanite and sillimanite-orthoclase zones were reached. The low slope and prograde character of the paths suggest a strong heat source, and Arenas and Martínez Catalán [2003] suggested that a detachment underlay the deep parts of the footwall unit, because isobaric heating may occur in the hanging wall to extensional detachments. We will see that these paths and the presence of an underlying detachment are not supported by the thermal models.

Sanabria dome

The metamorphic evolution was studied by Díez Montes [2007] and is summarised in figure 3B (arrows J to M). The evolution does not differ greatly from that of the Lugo dome, but in Sanabria, the voluminous Ollo de Sapo Fm, of quartzo-feldspathic composition, makes it difficult to trace several of the isograds as they are characteristic of metapelites. A garnet zone cannot be traced, although this phase is common in the sillimanite-orthoclase zone. As in the Mondoñedo nappe, kyanite occurs only in a few points of the biotite zone, and as a relict phase in the sillimanite-orthoclase zone

Four P-T paths were drawn by Díez Montes [2007] for different metamorphic zones using the same petrogenetic grid as for the Mondoñedo nappe and thermobaric calculations. Two of them (K and L) are for the same stratigraphic level, Early Ordovician slates, but in the northern and southern limbs of the dome respectively. Note that only the biotite zone was reached in the north whereas the south went into the sillimanite zone.

The initial prograde path is considered of somewhat lesser pressure than in the Mondoñedo nappe, due to the scarcity of garnet, but in a given moment, the Sanabria region was buried and kyanite grew in Early Ordovician aluminous slates of the biotite zone. This was probably due to the emplacement of the allochthonous complexes and is marked by a step in paths K and M. Deep parts of the dome were subsequently decompressed, entering the sillimanite-orthoclase zone and undergoing retrogression through the andalusite zone (path M) during extension and thinning. Temperatures obtained there using thermobarometry range between 500 and 650 ºC. Upper parts sustained apparently no decompression, and were heated reaching the sillimanite zone before undergoing retrogression (path L). According to Díez Montes [2007], paths L and M would reflect respectively upper and lower levels of the E1 shear zone, demonstrating its extensional character (fig. 2).

GRANITE INTRUSIONS

Three main groups of Variscan granitoids occur in Northwest Iberia [Capdevila, 1969; Capdevila and Floor, 1970]. The oldest consists of metaluminous, biotite-rich synkinematic granodiorites, poor in fluid phases and showing tonalitic facies and enclaves. They are allochthonous in relation to their country rocks, derive from partial melting of the lower crust [Capdevila, 1969], and include a mantle contribution [Galán *et al.*, 1996]. The crystallisation age of one of them in the Lugo dome is 323^{+9}_{-5} Ma [Fernández-Suárez *et al.*, 2000], so that, by that time, the temperature reached by the

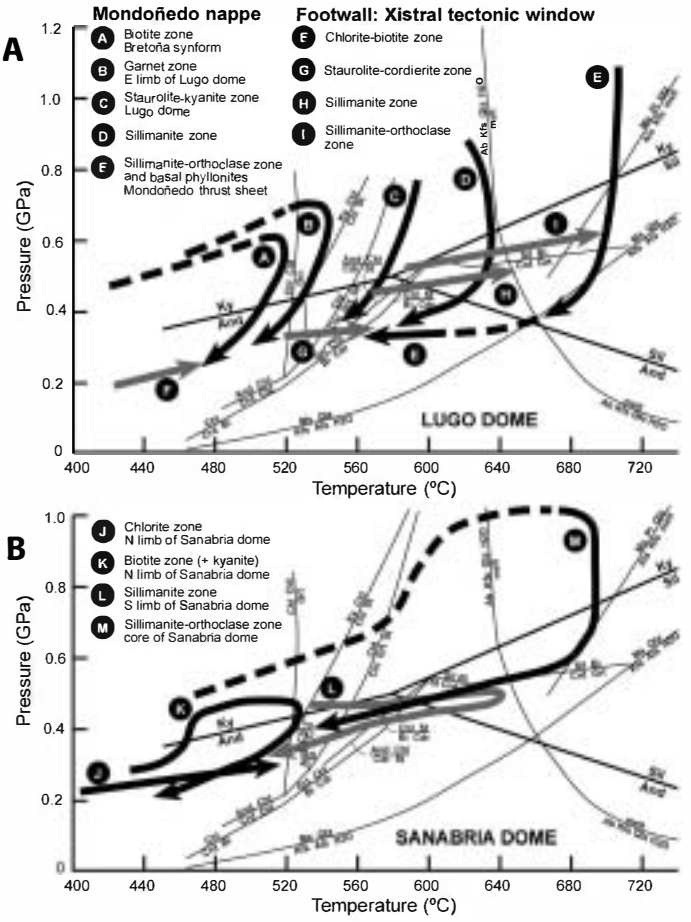

FIG. 3. – P-T paths for the Lugo dome (A), and the Sanabria dome (B), after Arenas and Martínez Catalán [2003] and Díez Montes [2007] respectively. Curves of mineral equilibrium according to Powell and Holland [1990] for the pelitic system, and to Luth *et al.* [1964], Le Breton and Thompson [1988] and Chatterjee and Johannes [1974], for the minimum melting in the hydrous granitic system, and for the disappearance of muscovite. The location of the different paths is shown in figure 2.

FIG. 3. – *Trajectoires P-T pour les dômes de Lugo* (A) *et Sanabria* (B), *d'après Arenas et Martínez Catalán [2003] et Díez Montes [2007] respectivement. Courbes d'équilibre selon Powell et Holland [1990] pour le système pélitique, et selon Luth* et al. *[1964], Le Breton et Thompson [1988] et Chatterjee et Johannes [1974], pour la fusion minimale dans le système granitique hydraté et la disparition de la muscovite. La position des trajectoires est marquée sur la figure 2.*

lower crust should have been high enough to generate tonalitic melts, probably by melting of biotite and/or amphibole.

The second group consists of synkinematic, peraluminous, two-mica granites, rich in fluid phases and metasedimentary enclaves. They derive from metasediments, and their character vary from subautochthonous to allochthonous in relation to the country rocks. Two U-Pb ages of 317^{+9}_{-5} Ma and 313 ± 2 Ma were obtained by Fernández-Suárez *et al.* [2000] in massifs of the Lugo dome. In this case, the middle crust should have reached the temperature necessary to generate melts of granitic (monzogranites, adamellites) composition at that time, probably by melt-producing reactions driven by the decomposition of muscovite.

The third group includes a wide range of compositions, from granodiorite to monzogranite and adamellite, with the common characteristic of being postkinematic and clearly allochthonous, often intruding in upper crustal levels. Postkinematic granitoids have been dated by the U-Pb method

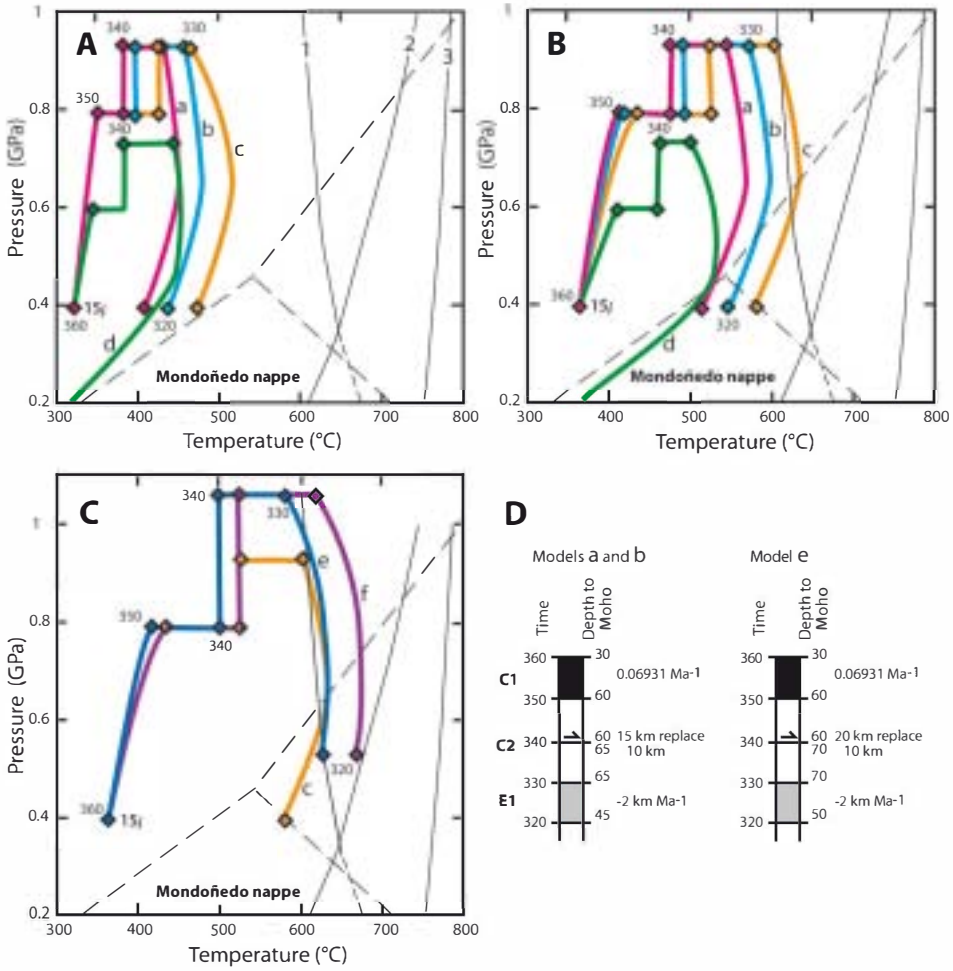

FIG. 4. – Thermal models of the Mondoñedo nappe used to identify general conditions consistent with geological data. – A: radiogenic heat production evenly distributed through the upper 15 km, contributing to the surface heat flux with 30 mW m^{-2}. P-T-t paths follow the temperature change in rocks initially 15 km deep (15*i*) that underwent: a– homogeneous thickening of entire lithosphere, b– thickening limited to the crust, c– thickening limited to upper 20 km of crust, all by a factor of 2; and d– thickening of upper 20 km by a factor of 1.5. The allochthonous complexes are 15 km thick and replace the upper 10 km of the footwall. – B: similar to A, but with a contribution of 40 mW m^{-2} to surface heat flux. – C: radiogenic heat production with flux of 40 mW m^{-2} at the surface, and homogeneous thickening by factor of 2. In paths e and f the allochthon is 20 km thick and replaces upper 10 km of footwall. In path e the entire crust is thickened while in f thickening is limited to the upper 20 km; c– repeats model c from previous figure. Points on the paths indicate time intervals of 10 Ma. Reactions curves are 1: pelite minimum melt, 2: muscovite dehydration melting [Thompson, 2001], 3: biotite dehydration melting [Le Breton and Thompson, 1988]. Stability fields for the aluminosilicate polymorphs according to Powell and Holland [1990]. – D: model structural changes through time are presented as a record of crustal thickness (depth to the Moho in km), timing of orogenic events (age in Ma), and strain rates (see text). Only models a, b, and e have been represented. Similar model representation is used in figures 5, 6 and 8.

FIG. 4. – *Modèles thermiques de la nappe de Mondoñedo utilisés pour établir les conditions générales en concordance avec les données géologiques.* – A : *chaleur radiogénique produite de façon homogène dans les 15 km supérieurs, contribuant au flux de chaleur à la surface pour 30 mW m*$^{-2}$. *Les trajectoires P-T-t montrent l'évolution thermique des roches qui étaient à l'origine à 15 km de profondeur (15i), et ont subi :* a– *épaississement de toute la lithosphère,* b– *épaississement limité à la croûte,* c– *épaississement limité aux 20 km supérieurs de la croûte, tous par un facteur de 2, et* d– *épaississement des 20 km supérieurs de la croûte par un facteur de 1,5. Les complexes allochtones ont une épaisseur de 15 km et remplacent les 10 km supérieurs de l'autochtone relatif.* – B : *comme A mais avec une contribution au flux de chaleur à la surface de 40 mW m*$^{-2}$ *et* – C : *chaleur radiogénique produisant un flux de chaleur à la surface de 40 mW m*$^{-2}$ *et un épaississement homogène par un facteur de 2. Dans les trajectoires e et f, l'allochtone a 20 km d'épaisseur et remplace 10 km d'autochtone. Dans e, toute la croûte a été épaissie, tandis que dans f, l'épaississement est limité aux 20 km supérieurs ;* c– *est comme le modèle c de la figure précédente. Les points sur les trajectoires indiquent des intervalles de 10 million d'années. Les courbes des réactions sont 1 : fusion minimale des pélites, 2 : fusion avec déshydratation et disparition de muscovite [Thompson, 2001], 3 : fusion avec déshydratation et disparition de biotite [Le Breton et Thompson, 1988]. Champs de stabilité des silicates d'aluminium d'après Powell et Holland [1990].* – D : *les changements structuraux dans les modèles à travers du temps sont représentés comme un enregistrement de l'épaisseur crustale (profondeur du Moho en km), âge des événements orogéniques (en million d'années) et vitesses de déformation (voir texte). Seulement les modèles a, b et e ont été représentés. On utilise la même représentation*

between 295 and 285 Ma [Fernández-Suárez *et al.*, 2000], and by the $^{40}Ar/^{39}Ar$ method between 285 and 275 Ma [Dallmeyer *et al.*, 1997]. U-Pb data are considered more reliable for crystallisation ages.

Granite generation in an orogenic context implies that the continental crust is hot enough as to undergo partial melting. A hot crust is also the condition required to initiate the extensional collapse [England and Thompson, 1986; Burg *et al.*, 1994]. Consequently, timing of granite emplacement is an important tool to test the validity of numerical models. Furthermore, Galán *et al.* [1996] have found a mantle contribution in the first group of granitoids, whereas Fernández-Suárez *et al.* [2000], have proposed that the third group of granitoids result from delamination at the end of the Variscan Orogeny. Thermal modeling may estimate the need of mantle involvement and its extent.

THERMAL CONSTRAINTS

According to England and Thompson [1984], thermal equilibrium in passive continental margins is reached in about 60 Ma. In Northwest Iberia, thermal relaxation took place between the intrusion of Early Ordovician granitoids [470 Ma; Lancelot *et al.*, 1985; Valverde-Vaquero and Dunning, 2000] plus very limited Silurian volcanism [420 Ma; Ancochea *et al.*, 1988], and the first Variscan deformation event [360 Ma]. Consequently, we may consider that the crust had been thermally re-equilibrated before the onset of the Variscan collision. The thick Cambrian to Early Devonian platform-facies succession indicates thermal subsidence, confirming cooling of the margin prior to the orogeny.

For the heat flow, a value of 60 mW m^{-2} is suggested by England and Thompson [1984] for the Neoproterozoic and Paleozoic continental crust, with 30 mW m^{-2} supplied by the mantle and 30 mW m^{-2} originated in the upper 15 km as radiogenic heat. More precisely, Fernández *et al.* [1998] have found a mean heat flow of 71 mW m^{-2} for the Iberian Massif, the Variscan basement of Iberia. These authors also calculated the rate of radiogenic heat production in basement rocks, with values between 1.5-3.5 μW m^{-3} in metasediments of the autochthon of Northwest Iberia (mean of 2.25 μW m^{-3}) and 0.9-4.7 μW m^{-3} in granitoids of the whole Iberian Massif (mean of 3.26 μW m^{-3}). Assuming constant heat production in the uppermost 15 km of crust, the radiogenic contribution to the heat flow there will be of 35 mW m^{-2} for the metasediments and 50 mW m^{-2} for the granitoids. As Variscan granitoids are the product of reworking of older crust, and no new radiogenic sources were incorporated to the autochthon during or after the Variscan Orogeny, the present high radiogenic contribution can be extrapolated to the time of Variscan deformation.

Accordingly, a value of 70 mW m^{-2} is reasonable for the autochthonous continental crust at the time of Variscan deformation, with 30 mW m^{-2} supplied by the mantle and 40 mW m^{-2} originated in the crust. Tests were carried out using either a homogeneous distribution of heat production in the upper 15 km of the crust, or an exponential decrease in heat production with depth for the whole crust. The thermal evolutions were similar, suggesting that the way in which the radiogenic heat production decreases with depth does not affect the models very much, providing that it is high in the upper crust and zero at its base. Much more important is the total heat flux delivered to the surface. The final models used homogeneous heat production in the upper 15 km, which corresponds to a mean radiogenic heat production of 2.67 μW m^{-3} in the upper crust.

The allochthonous complexes include abundant metasediments and granitoids, sources of radiogenic heat production, but as they consist also of lower crustal units, ophiolites, and mantle, their contribution may be smaller. A value of 55 mW m^{-2} will be taken, 25 mW m^{-2} of which derived from radiogenic heat.

Other parameters have been chosen as follows. For the thermal conductivity of the crust, a value of 2.25 W m^{-1} K^{-1} has been used based on England and Thompson [1984]. The arithmetic mean of 68 values measured in wells of the Iberian Massif yields 2.86 W m^{-1} K^{-1} [Fernández *et al.*, 1998], but these correspond to the present crystalline basement, quite different to the sedimentary pile existing at the beginning of Variscan deformation. For the mantle, we use a value of 3.3 W m^{-1} K^{-1} [Turcotte and Schubert, 1982]. The specific heat capacity of rocks is assumed to be 1000 J kg^{-1} K^{-1} [Turcotte and Schubert, 1982; Peacock, 1989; Stüwe, 2002], whereas the densities of crust and lithospheric mantle have been fixed at 2700 kg m^{-3} (upper crust), 2900 kg m^{-3} (lower crust) and 3260 kg m^{-3} (mantle). With these values, thermal diffusivity is 8.33 x 10^{-7} m^2 s^{-1}, 7.76 x 10^{-7} m^2 s^{-1}, and 1 x 10^{-6} m^2 s^{-1} respectively. Finally, the bottom of the lithosphere has been placed to coincide with the 1300 °C isotherm, based on Parsons and McKenzie [1978], and McKenzie and Bickle [1988]. Details of parameters used are given in table I.

STRAIN RATES AND DEFORMATION-TIME SCHEMES

Our aim is not to improve the methodology to carry out thermal modeling as established by England and Thompson [1984] and Peacock [1989], but to apply it to real cases. However, as in the real world deformation is not instantaneous, and we have some time constraints available, we introduce homogeneous progressive deformation in our models instead of the instantaneous crustal thickening used by the pioneers.

When ductile deformation is involved in the models, thickening or thinning during a given time interval can be incorporated by using a strain rate. For one dimensional models, only changes in the length of vertical lines must be considered. The parameter commonly used is the elongation (e), defined as the change in length of a line in relation to its original length: $e = (l_f - l_0)/l_0$, where l_0 and l_f are the initial and final lengths respectively [Means, 1976].

However, for progressive deformation, elongation increments must be considered, and the smaller the increments, the better is the value obtained for the finite strain. The most precise option is to use a parameter called natural strain, which is an integrated infinitesimal elongation [Means, 1976]: $\bar{e} = \int dl/l = \ln(l_f/l_0) = \ln(1+e)$.

The natural strain rate then will be:

$\dot{e} = \ln(l_f/l_0)/\Delta t = \ln(1+e)\Delta t$

As $\ln(l_f/l_0) = \Delta t \cdot \dot{e}$, the depth of any point after a finite time interval (Δt) will be: $l_f = l_0 \cdot \exp(\dot{e} \cdot \Delta t)$, or $z = z_0 \cdot \exp(\dot{e} \cdot \Delta t)$ when calculated using the initial depth (z_0) and the time passed since deformation started. Using the

TABLE I. – Model parameters
TABL. I. – *Paramètres des modèles*

Thermal conductivity	2.25 W m^{-1} K^{-1} (crust), 3.3 W m^{-1} K^{-1} (mantle)
Thermal diffusivity	8.33 x 10^{-7} m^2 s^{-1} (upper crust), 7.76 x 10^{-7} m^2 s^{-1} (lower crust), 1.0 x 10^{-6} m^2 s^{-1} (mantle)
Radiogenic heat production, upper crust	2.67 μW m^{-3}
Radiogenic heat flux at surface	40 mW m^{-2} (autochthon; some models use 30), 25 mW m^{-2} (allochthonous complexes)
Heat flux from the asthenosphere	30 mW m^{-2}
Surface temperature	25 °C
Density	2700 kg m^{-3} (upper crust), 2900 kg m^{-3} (lower crust), 3260 kg m^{-3} (mantle)
Initial thickness of crust	30 km
Initial thickness of radiogenic crust	15 km
Initial thickness of lithosphere	86 km (depth where T > 1300 °C)
Initial homogeneous thickening factor	1.5 or 2.0
Thickness of overthrusts (allochthonous complexes and Mondoñedo nappe)	10 to 20 km that replace 10 km of footwall
Distance between nodes	1000 m
Time step	1000 a

depth before the last increment (z_{n-1}), the new depth will be: $z_n = z_{n-1} \cdot \exp(\dot{e} \cdot \Delta t)$, with Δt now being the time interval between successive increments. We have used time increments of 1000 years in the models.

Progressive ductile deformation is shown in the time schemes that accompany the results of numerical models by a time interval filled in black for crustal thickening and grey for crustal thinning, and by the value of the natural strain rate ($\dot{e}$) in Ma^{-1}. For instance, 0.06931 Ma^{-1} means that a crust 30 km thick doubles its thickness in 10 million years: $\dot{e} \cdot \Delta t = 0.06931 \cdot 10 = 0.6931$, and $30 \cdot \exp(0.6931) = 60$ km.

For thrusting, the effect of heating induced by the thrust sheet in its footwall unit is difficult to model in a progressive way. For that reason, thrusts are modelled as instantaneous, following England and Thompson [1984], and a time for thermal relaxation will be included before or/and after thrusting, to compensate for the fact that thrust motion actually occurs along a finite time interval. Shear heating is not contemplated.

England and Thompson [1984] modelled thrusting by adding the thrust thickness to the previous thickness of the crust. This would be correct for thrusts using the Earth surface to glide, but most thrusts are dipping faults intersecting Earth surface at their fronts, where thrust sheets are supposed to be eroded as they move. In our case, the proof that neither the allochthonous complexes, nor the Mondoñedo nappe were thrust over the Earth surface is that their relative autochthons had previously reached the chlorite zone and had developed the S_1 cleavage. This implies that thrusting carried deep rocks to a higher position, and that rocks initially above the present autochthon were removed by the same thrust fault. For that reason, we will use a replacement mode for thrusts. The change in depth of any point or node below the thrust will be given by: $z_n = z_{n-1} + \Delta c$, where Δc is the added thickness in km, which equals the thickness of the thrust sheet minus the thickness of the footwall crust it replaces. Thrusts are shown in the time schemes by a line with an arrow, and indicated by an expression like "20 km replace 10 km", meaning that a thrust sheet 20 km thick replaces 10 km of its footwall, adding only 10 km of overburden.

Normal detachment faults do not include any external heat source, as is the case for thrusts, because a portion of crust is subtracted from the modeled vertical column instead of being added. Their motion can be modelled as progressive, simply changing the depths below them according to: $z_n = z_{n-1} - u \cdot \Delta t$, where $-u$ is the rate of uplift or exhumation. No changes in depth occur above the fault, and nodes initially below it are eliminated as they become shallower than fault depth. Normal detachments are indicated in the time schemes by a grey filling (the same as for extensional ductile deformation), and by the exhumation rate in km per million years (e.g.: –1 km Ma^{-1}). The expression "z >10 km" indicates that fault depth is 10 km and only points beneath that depth move upwards.

Finally, progressive erosion can be modeled in the same way as the footwall to extensional detachments, with the same equation: $z_n = z_{n-1} - u \cdot \Delta t$ but applied to all depths. In that case, the exhumation rate in km per Ma is indicated.

MODELING PROCEDURE

Thermal regimes and their change through time have been calculated using a one-dimensional finite-difference model [Peacock, 1989, 1990, 1991] that tracks position and temperature of nodes during deformation and the thermal response to deformation. For the models tested, an initial geotherm for a 30 km thick crust was calculated using a heat flux of 30 mW m^{-2} from the asthenosphere to mantle lithosphere and an additional 40 mW m^{-2} (or rarely 30 mW m^{-2}) delivered to the surface as heat generated by decay of radiogenic elements distributed evenly through an upper layer of the crust, initially 15 km thick. This results in a surface heat flux of 70 mW m^{-2}.

The model crust is then subjected to a series of deformations that include homogeneous thickening (to simulate C1 crustal thickening contemporaneous with recumbent folding) and overthrusting replacing a portion of the crust (to model C2, the emplacement of the allochthonous complexes and the Mondoñedo nappe). Thickening is followed

by thermal relaxation and then by homogeneous thinning (E1 extensional ductile shear zones) that returns the Moho to a depth of between 40 and 50 km. In addition, 5 km of crust is removed by an upper-crustal detachment (E2, simulating the Viveiro and Chandoiro faults) in some models. In most models only the crust is thickened; however, in all cases thinning is assumed to affect the entire lithosphere.

We prefer to model deformations such as homogeneous thickening and thinning as processes that occur at rates consistent with geological strain and have modelled and tracked model movements using natural strain. This approach tends to produce P-T-t paths with a more realistic appearance than those that result from models that use instantaneous change. However, the end result, that is thermal

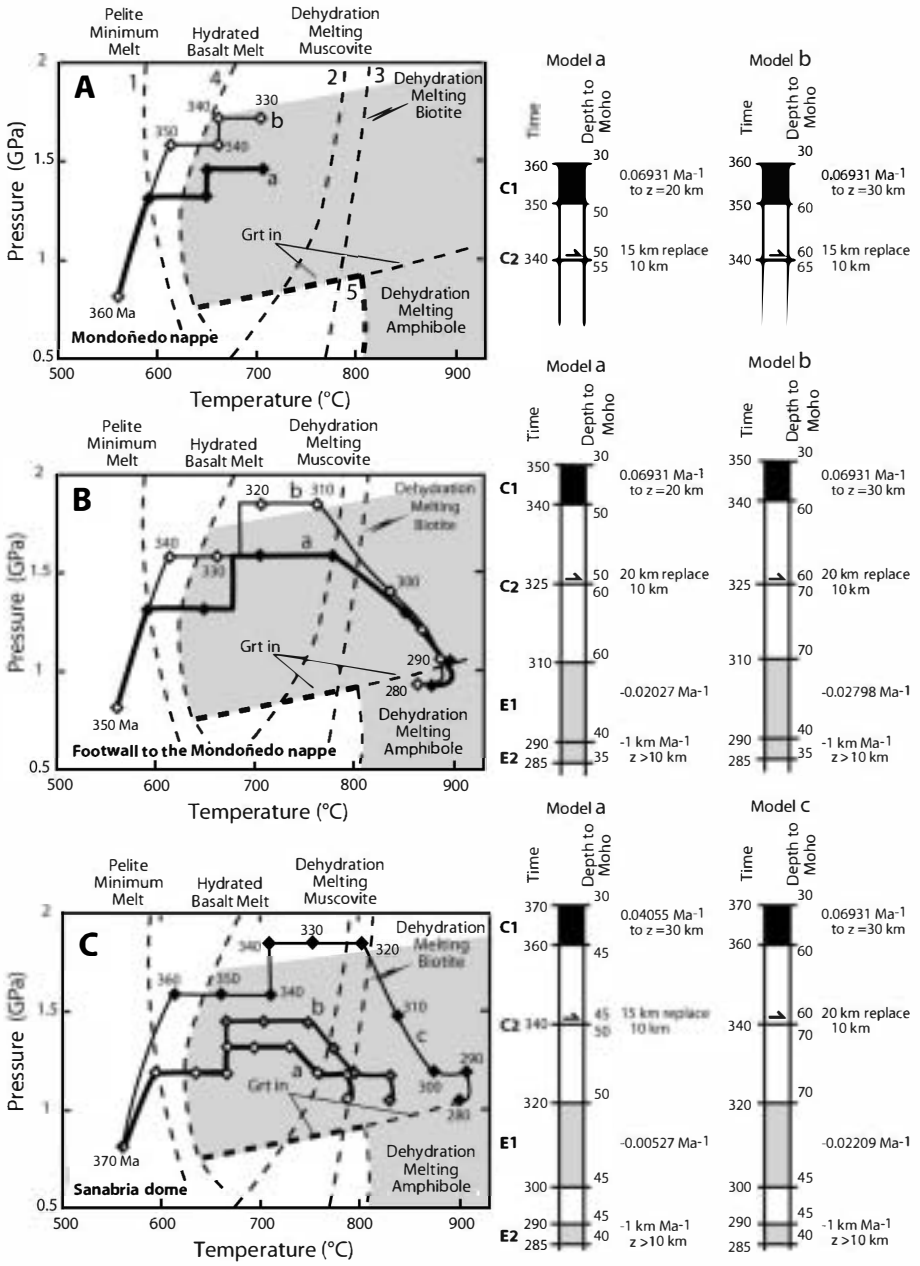

FIG. 5. – Model results showing the thermal effect of thickening on the Moho. Dynamo-thermal models intended to represent orogenic thickening and thinning should be consistent with the production of lower crustal melts (grey area) at model times of 30 and 60 Ma.– A: Mondoñedo nappe.– B: Footwall to the Mondoñedo nappe at the Xistral tectonic window, Lugo dome.– C: Sanabria dome. Structural changes during orogeny are given to right of model results. Model b in C is similar to model a, but with a 20 km thick allochthon replacing the upper 10 km of crust at its footwall. Reaction curves 1, 2, and 3 as in figure 4. Other reactions are 4: melting of basalt, and 5: dehydration melting field for amphibole and the garnet-in reaction for basaltic amphibolites [Rapp and Watson, 1995]. In this and the following figures, radiogenic heat production is initially distributed through the upper 15 km, contributing to the surface heat flux with 40 mW m^{-2}, and time is shown in Ma only for the P-T-t path reaching the highest pressure.

FIG. 5. – *Modèles montrant l'effet thermique de l'épaississement dans le Moho. Les modèles dynamo-thermiques simulant l'épaississement et l'amincissement orogéniques doivent fournir la production des liquides dans la croûte inférieure après 30 et 60 Ma.* – A : *nappe de Mondoñedo.* – B : *autochtone de la nappe de Mondoñedo dans la fenêtre tectonique de Xistral, dôme de Lugo.* – C : *dôme de Sanabria. L'histoire structurale pendant l'orogenèse est montrée à droite. Le modèle b dans C est comme le modèle a sauf que 20 km d'allochtone remplacent les 10 km supérieurs de l'autochtone relatif. Courbes des réactions 1, 2 et 3 comme sur la figure 4. D'autres réactions sont 4 : fusion du basalte, et 5 : fusion avec déshydratation pour amphibole et la réaction produisant du grenat dans des amphibolites basaltiques [Rapp et Watson, 1995]. Dans cette figure et les figures suivantes, la chaleur radiogénique est au début distribuée de façon homogène dans les 15 km supérieurs, contribuant au flux de chaleur à la surface pour 40 mW* m^{-2}. *Le temps est montré seulement pour la trajectoire atteignant la plus haute pression.*

conditions in the lithosphere, is little changed by this aspect of the models and within a few million years resulting differences are small and are within error introduced by estimates of parameters used to compute thermal relaxation and estimates of the timing of deformational events based on geochronology.

For initial crustal thickening, we have used age data of Dallmeyer *et al.* [1997] and taken into account the diachronous character of C1 deformation. We have considered an interval of 10 Ma for this event, and progressive younging toward the external zones: 370-360 Ma in Sanabria, 360-350 Ma in the Mondoñedo nappe and 350-340 Ma in its autochthon.

We have treated thrusting as an instantaneous event. Emplacement of the allochthonous complexes above the Mondoñedo nappe and above the autochthon of the Sanabria dome has been modelled at 340 Ma. The properties of the thrust sheet are those of a continental crust with an equilibrium geotherm. For the emplacement of the Mondoñedo nappe we have considered an instantaneous event at 325 Ma, with the base of the nappe being 35 km deep prior to thrusting, according to geothermobarometry estimations [Reche *et al.*, 1998]. Because maximum pressures experienced by footwall rocks near the base of the nappe were less than 0.6 GPa, the nappe must have experienced significant thinning during emplacement either by erosion or tectonic denudation. To include the thermal changes during thinning in the emplacement model, we have chosen to model the thinning as rapid erosion (removal of the upper portions of the crust at a rate of 1.5 mm per year). At this rate, rocks

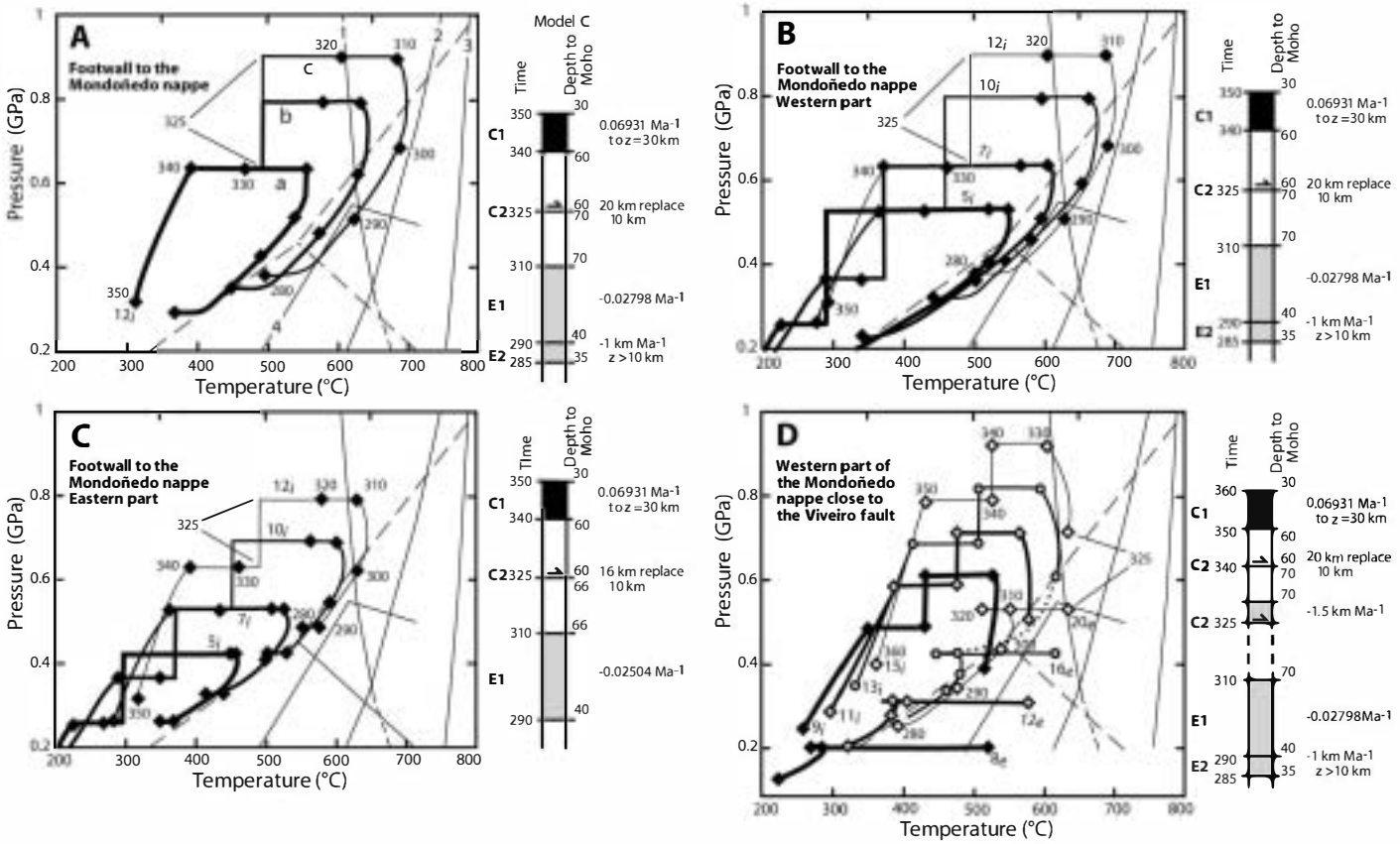

FIG. 6. – P-T-t paths for rocks originating at different depths and in different locations within the Lugo dome. – A: three models of the Mondoñedo nappe for rocks at its footwall, shown for rocks at an initial depth of 12 km: a– 10 km thick nappe, b– 16 km thick nappe, and c– 20 km thick nappe, in all cases replacing 10 km of its footwall.– B: P-T-t paths for footwall rocks initially at depths of 5, 7, 10, and 12 km, with 20 km of nappe replacing 10 km of footwall. Results are consistent with P-T-t paths inferred for the western part of the autochthon in the Xistral tectonic window. – C: as previous, but with a 16 km thick nappe, consistent with metamorphism of the eastern parts of the window, and implying that the nappe thinned towards its front. – D: model results for the western part of he Mondoñedo nappe close to the Viveiro fault. Every P-T-t path is shown in two parts, before and after thrusting. The paths for rocks initially at 9, 11, 13, and 15 km (e.g. 9*i*) are followed until the time of nappe emplacement at 325 Ma. After, paths for the same rocks, that were at depths of 8, 12, 16, and 20 km within the nappe at the time of its emplacement (e.g. 8*e*) are shown. Reaction curves 1, 2, and 3, as in figure 4. Curve 4 : approximate boundary for cordierite stability as determined for the KFMASH system [Spear *et al.*, 1999].

FIG. 6. – *Trajectoires P-T-t pour des roches qui étaient à l'origine à des profondeurs différentes et dans des lieux différents dans le dôme de Lugo.* – A : *trois modèles de la nappe de Mondoñedo pour des roches de son autochtone relatif qui étaient à l'origine à une profondeur de 12 km. L'épaisseur de la nappe est de :* a– *10 km,* b– *16 km, et* c– *20 km, et remplace dans les trois cas les 10 km supérieurs de l'autochtone relatif.*– B : *trajectoires P-T-t pour des roches de l'autochtone relatif qui étaient à l'origine à des profondeurs de 5, 7, 10 et 12 km, avec 20 km d'épaisseur de la nappe remplaçant 10 km de l'autochtone relatif. Les résultats sont en accord avec les trajectoires établies dans la partie ouest de la fenêtre tectonique de Xistral.* – C : *comme B mais avec 16 km d'épaisseur de la nappe, en accord avec le métamorphisme de la partie est de la fenêtre tectonique, ce qui implique que la nappe s'amincissait vers son front.* – D : *résultats du modèle de la partie ouest de la nappe de Mondoñedo prés de la faille de Viveiro. Chaque trajectoire P-T-t est montrée en deux parties, avant et après le chevauchement. Les trajectoires pour des roches à des profondeurs de 9, 11, 13, et 15 km à l'origine (p. ex. 9i) sont suivies jusqu'à la mise en place de la nappe il y a 325 Ma. Ensuite, on montre les trajectoires des mêmes roches, qui étaient à 8, 12, 16 et 20 km de profondeur dans la nappe (p. ex. 8e) au moment de sa mise en place. Courbes des réactions 1, 2 et 3 comme sur la figure 4. Courbe 4 : limite de stabilité de la cordiérite pour le système KFMASH [Spear* et al., *1999].*

15 km deep would reach the surface in 10 Ma. The geotherm created by 5 Ma of erosion is then used to model the impact of the thrust on the thermal history of the footwall rocks. We think that this average geotherm is a reasonable approximation of the thermal regime of the hanging wall during its emplacement. We have tested this inference by using alternative geotherms including pre- and post-erosional geotherms among others and found that the geotherm of the hanging wall is rapidly changed and has little impact on the P-T-t path of the footwall.

RESULTS AND DISCUSSION

General

Tectono-thermal histories derived from one-dimensional finite-difference models of thickened and thinned crust are presented in figures 4 through 8. They are organized so as to present the models that best conform to known constraints on thermal histories for each of the three crustal packages studied.

First considered are models representing the Mondoñedo nappe as the one that places greatest constraints on the values of model parameters. This is because it requires rapid heating of mid crustal rocks to conditions consistent with sillimanite and sillimanite-orthoclase bearing metamorphic assemblages and partial melting of the lower crust in a similar time frame. Two key facts emerge from efforts to model the nappe (figs. 4, 5). First, the Iberian crust involved in the Variscan orogeny was relatively rich in radiogenic elements so that the heat flux produced by those elements at the surface approached or exceeded 40 $mW \cdot m^{-2}$. Comparing results using a radiogenically derived flux of 30 and 40 $mW \cdot m^{-2}$ (figs. 4A, 4B), one sees that temperatures during thermal relaxation of a crust with lower radiogenically derived heat flux reaches neither the first nor second sillimanite isograds within constraints inferred from structure and geochronology. However, in figure 4B, models b and c both reach sillimanite isograd in 35 Ma and model c achieves temperatures consistent with anatexis and the production of sillimanite-orthoclase bearing assemblages.

Because models employ a two-layered crust with respect to the concentration of radiogenic elements, each layer initially 15 km thick, we estimate radiogenic heat production in the upper crust to have been approximately 2.7 $\mu W \cdot m^{-3}$. This relatively high heat production is consistent with measured heat flow from the Northwest Iberian peninsula [Fernández *et al.*, 1998] and with observed crustal lithologies, consisting mostly of terrigenous metasediments, pre-Variscan acid metavolcanic rocks (Ollo de Sapo Fm), and granitic orthogneisses. It is also within the range of values used by others in thermal modeling [e.g., England and Thompson 1986] and only 2/3 of the heat production used and considered reasonable in models presented by Gerbi *et al.* [2006]. According to this first result, a surface heat flux of 70 mW m^{-2}, with radiogenic heat generated through the upper 15 km and contributing 40 mW m^{-2} of the surface heat flux will be used in all of the following models.

The second result of importance inferred from the model outcomes presented in figure 4 is that thickening must have been limited to the crust and possibly to the middle and upper crust. Homogeneous thickening of the entire

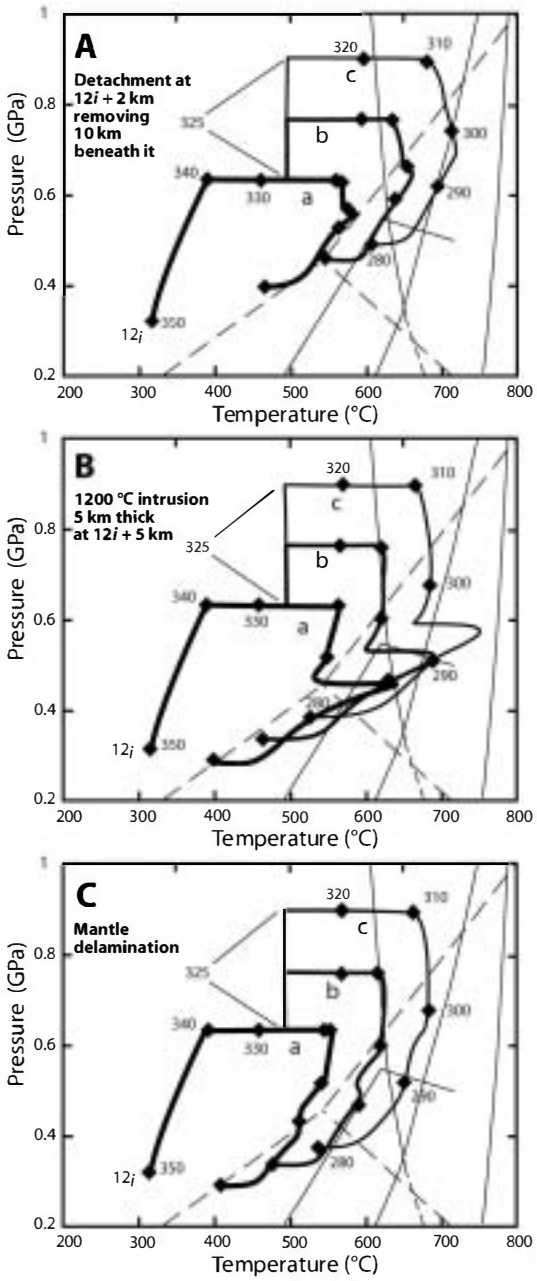

FIG. 7. – Alternative models for the footwall to the Mondoñedo nappe. – A : an extensional detachment situated 2 km beneath rocks initially 12 km deep removes 10 km of crust under it. – B: a 5 km thick, 1200 °C mafic intrusion with its roof 5 km below rocks initially 12 km deep. – C: delamination moving 1300 °C asthenospheric rocks to the base of the crust. All the events are instantaneous and occurred at 295 Ma (55 Ma of model time). Three structural models are presented in each figure, all including homogeneous thickening by a factor of 2 in 10 Ma, and a different thickness for the Mondoñedo thrust sheet : a– 10 km, b– 15 km, and c– 20 km thick nappe, in all cases replacing 10 km of its footwall. Reaction curves as in figure 6.

FIG. 7. – *Modèles alternatifs pour l'autochtone relatif de la nappe de Mondoñedo.* – A : *une grande faille normale à faible pendage située 2 km au-dessous des roches qui étaient à l'origine à 12 km de profondeur fait disparaître 10 km de la croûte au-dessous d'elle.* – B : *une intrusion des roches basiques à 1200°C, avec 5 km d'épaisseur s'est mise en place 5 km au-dessous des roches qui étaient à l'origine à 12 km de profondeur.* – C : *la délamination au niveau du Moho place des roches de l'asthénosphère à 1300°C à la base de la croûte. Tous ces événements sont instantanés et ont lieu il y a 295 Ma (55 Ma du temps du modèle). Trois modèles structuraux sont montrés sur chaque figure, avec un épaississement homogène par un facteur de 2 en 10 Ma et des épaisseurs différentes pour la nappe de Mondoñedo de : a– 10 km, b– 15 km, et c– 20 km, remplaçant dans les trois cas les 10 km supérieurs de l'autochtone relatif. Courbes des réactions comme dans la figure 6.*

lithosphere will not move mid-crustal rocks to sillimanite grade in 30 to 40 Ma (model a, figs. 4A, 4B). If thickening is limited to the crust sillimanite and sillimanite-orthoclase grade conditions can be reached in the allotted time frame if the emplacement of the allochthonous complexes increases crustal thickness by ≈ 10 km, a pressure increase ≈ 265 MPa (compare model b in fig. 4B and model e in fig. 4C). Alternatively, thickening only the upper 20 km of the crust produces higher temperatures and so will result in anatexis within rocks initially at a depth of 15 km if the thrust sheet increases crustal thickness by 5 km (≈ 130 MPa; see model c in figs. 4B and 4C). The models, therefore, suggest that petrological and rheological differences between crust and mantle (or between upper crust and a basic granulitic lower crust) produced a major crustal discontinuity during the Variscan collision, so that the denser, more competent rocks of the mantle (or perhaps lower crust) were detached and subducted while the middle and upper crust was thickened in response to its buoyancy-driven resistance to subduction.

These two findings, relatively high radiogenic heat production and thickening during the initial stages of compression limited to the crust, have been incorporated in the models that consider the thickening and thinning of the footwall rocks of the Mondoñedo nappe (Lugo dome) and the Sanabria dome.

A third result that emerges from the models of the Mondoñedo nappe is the ability of the lower crust to reach conditions that would produce anatexis required by the presence of granodioritic and subordinate tonalitic bodies that intruded the nappe and its footwall at 330-320 Ma [Fernández Suárez *et al.*, 2000], within 25 to 30 Ma of the onset of thickening. Figures 5A and 5B trace the thermal history for the base of the crust underneath the nappe and its footwall during model thickening and, in the case of the footwall, thinning. Figure 5C does the same for the Sanabria dome. As is evident in the figures, all models presented are able to produce at least limited melting of the lower crust through partial melting of hydrated pelites or andesitic to basaltic amphibolites aided by dehydration melting of amphibole within 25 Ma.

The footwall to the Mondoñedo nappe

Models intended to represent the detailed tectonothermal history of upper crustal rocks in the footwall to the Mondoñedo nappe are shown in figure 6. Figure 6A presents model results of the impact of different modes of nappe emplacement on rocks initially at a depth of 12 km. Models are for a Mondoñedo nappe 10, 16, and 20 km thick (models a, b, and c respectively) always replacing 10 km of its relative autochthon. Because rocks at the base of the nappe experienced a pressure of 0.9 GPa prior to thrusting [Reche *et al.*, 1998; Arenas and Martínez Catalán, 2003] and no record of similar high pressure is preserved in the assemblages of the footwall, the model treats the nappe as having been rapidly uplifted so that rocks that were at depths of 35 km prior to thrusting form the base of the nappe. The thermal structure of the thrust sheet is most commonly taken from models of the nappe (fig. 4) at 325 Ma, 35 Ma after initial thickening and 5 Ma after the initiation of exhumation and removal of the upper crust at a rate of 1.5 km Ma^{-1}. Nodes representing rock at depths of 7 to 27 km after 5 Ma of uplift are used to represent the thermal structure of the 20 km thick thrust (fig. 6D). Alternative models including a linear geotherm in the thrust sheet between 25 °C for the surface and 630 °C at the base, and rocks representing the upper 20 km of the nappe prior to uplift were also tested and found to have little impact on model results after a few million years of thermal relaxation.

Model results indicate that minor melting of the footwall rocks initially at a depth of 12 km occurs when the nappe thickens the crust by 6 km (model b, fig. 6A), and more significant melting would occur if the crust was thickened by 10 km (model c). If the nappe emplacement causes no net thickening (model a), then the rocks do not reach the sillimanite isograd.

Figures 6B and 6C illustrate the P-T paths for rocks at different initial crustal depths in the western and eastern parts of the Xistral tectonic window. In both, C1 represents homogeneous doubling of the crust between 350-340 Ma followed by emplacement of the Mondoñedo nappe at 325 Ma. The nappe was 20 km thick in the west and 16 in the east, and in both cases it replaces the upper 10 km of the footwall crust. Also included are the constraints inferred from the thermal history of the Mondoñedo nappe discussed above: limiting thickening to the crust and the inclusion of a crust with relatively high radiogenic heat production for the rocks of the footwall and the nappe.

For the western, higher-grade portions of the autochthon, key constraints on the model are the requirements that rocks that were initially at relatively high levels in the crust (8 to 10 km before initial thickening) reach sillimanite-orthoclase grade, and that anatectic reactions began by at least 315 Ma (35 Ma after initial thickening in the model). As is illustrated in figure 6B, these conditions are met as rocks that were initially at depths > 7 km cross the minimum melting curve for pelitic rocks before 310 Ma if initial homogeneous thickening doubles crustal thickness and the Mondoñedo nappe adds approximately 10 km of crust above the footwall. Note that when the nappe adds only 6 km of crust (fig. 6c), as modelled for the eastern part of the window, partial melting is reached only for rocks with an initial depth of > 11 km. Rocks higher in the model crust, representative of those now exposed along the eastern margin of the tectonic window, would not reach sillimanite isograde, would retain chlorite, and would barely pass through the andalusite stability field, results consistent with petrological observations.

However, differences between model results and prior interpretations of P-T paths for the Mondoñedo footwall [Arenas and Martínez Catalán, 2003] do arise, and become evident when comparing the grey arrows in figure 3A with model P-T-t paths of figures 6B and C. Previous interpretation of mineral associations inferred nearly isobaric heating of the footwall rocks, thought to be caused by advection of heat during exhumation of lower crustal rocks along a crustal-scale detachment zone [Arenas and Martínez Catalán, 2003]. Conversely, model results show that the P-T paths require a significant increase in pressure prior to heating and eventual passage through the sillimanite, sillimanite-orthoclase, and andalusite stability fields.

The presence of a buried detachment was thought to provide an explanation for the mineral assemblages indicative of low to moderate-pressure, high-temperature metamorphism, in particular the occurrence of sillimanite and

sillimanite-orthoclase without or with minor garnet, and the abundance of cordierite.

To test the detachment hypothesis, we have modelled the effect of an instantaneous detachment placed 2 km beneath rocks initially 12 km deep that removes 10 km of crust beneath it. Model results (fig. 7A) suggest that this interpretation is unlikely for two reasons. First, when a detachment is included in the model so that there is an instantaneous emplacement of high-temperature lower crustal rocks within one or two kilometres of the current topographic surface, advective heating does not have a major impact on peak temperatures reached in the rocks above the detachment. This result follows in part from the fact that the thermal gradient through the lower crust has been reduced by thermal relaxation and thinning before the modelled detachment and in part because the amount of crust that can be removed by the detachment is limited by constraints on maximum crustal thickness and the structural evidence for significant crustal thinning. As a result, the temperature increase resulting from advection on the detachment is likely to be no more than ≈ 20 °C (fig. 7A). Second, model results indicate that high-temperature metamorphism occurs when a thickened crust rich in radiogenic elements undergoes thermal relaxation. Important to the thickening is the emplacement of the thrust sheet, the increase in radiogenic sources within the crustal slice, and the pressure increase that results from its emplacement. As seen in the western and eastern parts of the Xistral tectonic window, relatively small changes in thickness of the thrust sheet have a significant impact on the resulting temperatures in the footwall. It follows that the most likely P-T path followed by the footwall rocks of the Lugo dome includes a significant increase in pressure followed by decompression during thermal relaxation.

Other two alternative sources of heat have also been considered, the intrusion of a 5 km thick mafic magmatic body at 1200 °C, roughly 5 km beneath the deepest outcropping rocks and delamination of the lithospheric mantle (figs. 7B, 7C). In each model some additional thickening is required if rocks that were initially at a depth of 12 km and reached 24 km during C1 are to reach temperatures consistent with partial melting. The intrusion of a large mafic magma body provokes a significant temperature increase, causing peak metamorphic conditions to cross into the cordierite stability field. This could partially explain the P-T paths deduced by Arenas and Martínez Catalán [2003], but this possibility is not supported by geophysical data, as gravity anomalies do not allow the presence of a large mafic body relatively near the surface beneath the Lugo dome [Ayarza and Martínez Catalán, 2007].

More surprising is the limited effect that mantle delamination has on the upper crustal rocks of the models. The effect is more to slow cooling but not to induce higher temperatures in rocks initially 12 km deep. Delamination cannot, therefore, have produced the isobaric heating inferred from mineral assemblages.

Although the scarcity of garnet remains puzzling, we suggest that it may reflect the relatively long time that the rocks remained at high temperature and low to moderate pressure in the presence of metamorphic fluids. Some whole rock chemistries favour aluminosilicate formation over garnet and the removal of garnet produced in the early

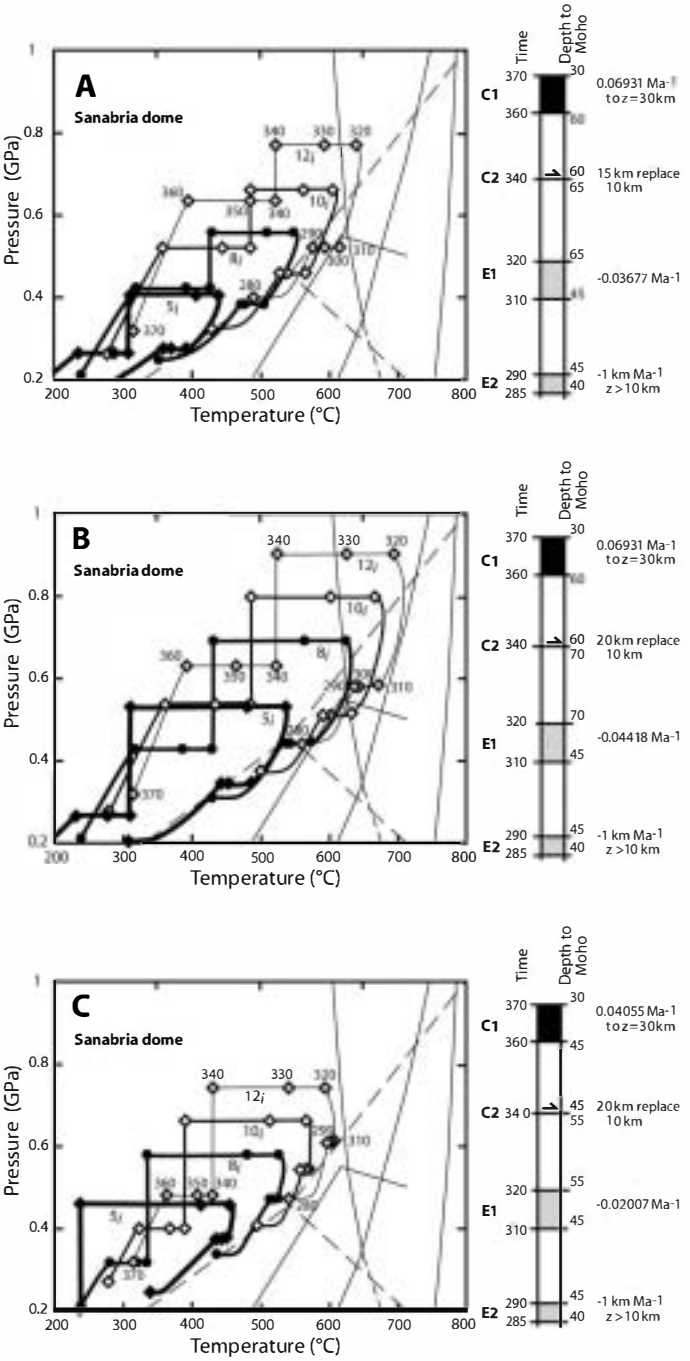

FIG. 8. – Model results for the Sanabria dome. – A: initial homogeneous thickening of the entire crust by a factor of 2 and emplacement of a 15 km thick allochthon replacing upper 10 km of its footwall. – B: same initial thickening and 20 km thick allochthon replacing 10 km of its footwall. – C: initial crustal thickening by a factor of 1.5 with a 20 km thick allochthon replacing 10 km of its footwall. Models A and B can be seen as representing the northern and southern limbs of the Sanabria dome respectively, except for the E2 event, only applicable in the south. The difference in thickness of the thrust sheet can be attributed to its tapering to the north, in the direction of nappe emplacement. Reaction curves as in figure 6.

FIG. 8. – *Résultat des modèles pour le dôme de Sanabria.* – A : *épaississement homogène de la croûte par un facteur de 2 et mise en place d'un allochtone de 15 km d'épaisseur remplaçant les 10 km supérieurs de l'autochtone relatif.* – B : *même épaississement initial et 20 km d'allochtone remplaçant les 10 km supérieurs de l'autochtone relatif.* – C : *épaississement homogène de la croûte par un facteur de 1,5 et 20 km d'allochtone remplaçant les 10 km supérieurs de l'autochtone relatif. Les modèles A et B sont représentatifs des flancs nord et sud du dôme de Sanabria respectivement, sauf pour l'événement E2, applicable seulement dans le sud. La différence en épaisseur de la nappe reflète son amincissement vers le nord, dans la direction de mise en place. Courbes des réactions comme dans la figure 6.*

stages of the prograde path through reactions that produce biotite and aluminosilicate. If equilibrium conditions near the metamorphic peak were such that garnet was unstable, then the long times involved in the thermal relaxation process and the presence of fluids, magmatic fluids in migmatites or hydrous fluids produced either by dehydration reactions or the crystallization of anatectic magma, might allow for full re-equilibration of assemblages. In this way any mineral record of higher pressures in the early stages of the P-T path might be lost.

The western part of the Mondoñedo nappe

General results for the Mondoñedo nappe are shown in figure 4 and described above. Detailed model results followed by points at different depths of the western part of the Mondoñedo nappe are illustrated in figure 6D, with particular emphasis in the evolution after nappe emplacement. The modeled instantaneous emplacement of the nappe results in unrealistic exhumation paths (dots for path 13i, fig. 6D), and are not continued beyond 325 Ma. After nappe emplacement, paths are shown for rocks within the nappe that where at depths of 8, 12, 16, and 20 km immediately after thrusting. Once post-thrust minimum temperatures are reached, the model should accurately portray the P-T path of the hanging wall. Of particular interest is the likely passage of rocks from sillimanite to kyanite or andalusite to kyanite before continued thermal relaxation reheats the deeper rocks of the nappe and returns them to the field of andalusite stability. Descriptions of the rocks in the hanging wall of the Viveiro fault, that preserves nappe rocks that were above the Xistral tectonic window, report just such a complex metamorphic history [Reche *et al.*, 1998].

The Sanabria dome

Results of several models using the inferred structural history of the rocks exposed in the Sanabria dome are presented in figure 8. Model P-T-t paths that indicate only very limited partial melting would occur if initial thickening is limited to 1.5 (fig. 8C). In contrast, doubling of the crust during initial thickening may produce temperatures too high and likely to produce more melting than is inferred to have occurred from migmatites exposed in the core of the dome (fig. 8B). We conclude that thickening was likely to have been by a factor between 1.5 and 2.0. If the emplacement of the allochthonous complexes added 10 km to the crust, causing a pressure increase $\approx$ 265 MPa in the Sanabria area, then thickening was probably closer to 1.5 than 2; however, if emplaced allochthon were thinner, then initial thickening must have approached a doubling of the crust (fig. 8A).

N-S differences in the Sanabria area, parallel to transport direction of the allochthonous units, reflect a marked decrease in metamorphic grade across the dome. Model results imply, as in the Xistral window, that these differences are caused by the decreasing thickness of the advancing thrust sheet so that overburden related to nappe emplacement decreased in the direction of transport. Once again a relatively small pressure difference (130 MPa or less) is enough to account for observed differences in metamorphic grade (figs. 8A, 8B). If figure 8B is considered to model the southern limb and figure 8A the northern limb, a decrease of 5 km of nappe thickness is inferred across a distance of $\approx$ 25 km. This translates into a dip of 11° for the thrust fault, very reasonable for the thrust of the allochthonous complexes near its frontal region.

Granitic and granodioritic magmatism

Thermal models provide a numerical explanation for the three distinct periods of Variscan magmatic activity in Northwest Iberia, characterized by three groups of granitoids: early granodioritic to tonalitic intrusions emplaced at $\approx$ 325 Ma, more voluminous leucogranitic intrusions crystallized between 315 and 310 Ma, and monzogranites and granodiorites intruded between 295 and 285 Ma [Capdevila, 1969; Capdevila and Floor, 1970; Fernández-Suárez *et al.*, 2000]. At least the two older pulses appear to move eastward through time, that is toward the foreland, reflecting the diachronous progress of deformation across the orogen [Bellido Mulas *et al.*, 1987].

Lower crustal melts produced by hydrous basaltic or andesitic amphibolites and amphibolite dehydration melting could produce granodioritic to tonalitic magmas within 25 to 40 Ma of initial crustal thickening (fig. 5). Production of these magmas is likely to be limited by availability of fluids and the temperature of the lower crust and so relatively small amounts of these intrusives would form. Shortly after this, rocks in the middle crust that initially were between 8 and 15 km deep, would become hot enough to cross reaction curves that produce melting in pelitic and or granitic rocks in the presence of hydrous fluids. Mostly leucogranitic magma would be produced through anatexis of these rocks. Volume of melt production would depend on the availability of fluid and peak temperatures reached, which in turn is dependent on the amount of crustal thickening. Decompression of the rocks during crustal thinning would allow additional melting in response to dehydration reactions even if fluids had been concentrated in the anatectic magmas.

Later melting would be dominated by the high temperature reached by the lower crust and so again would be mostly monzogranite to granodiorite. At about 300 Ma, 70 to 50 Ma after starting of crustal thickening, the lower crust would reach temperatures causing dehydration melting of biotite. These reactions as well as dehydration melting of amphibole, especially as temperatures increased to $\approx$ 900 °C, would produce the somewhat less silicic magmas that dominate the third, postkinematic pulse. The basic and ultrabasic rocks dated at 293^{+3}_{-2} Ma by Fernández-Suárez *et al.* [2000] may well reflect partial melting of the mantle. It is quite likely that as these magmas moved upward they might have generated limited secondary magmas if they rose through fertile crust.

This explanation of the magmatic postkinematic event in the Iberian Massif derived from thermal models removes the need that it be explained by mantle delamination [Fernández-Suárez *et al.*, 2000]. Although the result does not preclude delamination as a possible late-Variscan event, it does imply that the magmatic history of the region should not be used as evidence of such an event.

CONCLUSIONS

Finite-difference models of lithospheric thermal evolution can be used to validate the tectono-thermal evolution deduced

from structural, petrological, and geochronological data, to identify potential inconsistencies and errors, and to answer unresolved questions concerning orogenic mechanisms and modes of mantle involvement.

In the case of the late orogenic, extensional domes of Lugo and Sanabria, in Northwest Iberia, the models support the deformation scheme and show that timing, based on available isotopic data, may be correct. This is important for the main Variscan compressional events, for which data were scarce and based on a single source [Dallmeyer *et al.*, 1997].

Relatively high radiogenic heat production is necessary to explain the metamorphic evolution of the domes, but always within the reasonable limits of published present surface heat flow and radiogenic heat production of the Iberian Massif.

Thickening of the whole lithosphere during the first Variscan deformation event hinders the subsequent modeled thermal evolution from mimicking the observed metamorphic evolution. Temperatures are then lower than those necessary to reach sillimanite and sillimanite-orthoclase zones, and to pass through the andalusite field during exhumation. The models suggest that some kind of detachment occurred at the Moho or in the lower crust and that thickening only affected the crust or a part of it.

Large amounts of late-orogenic extension, based on wide extensional shear zones identified in the study area and modelled by vertical thinning, help model P-T-t paths to fit the metamorphic evolution of the domes, and in a way, validate the history deduced from geological criteria. In this case, vertical thinning affects the whole lithosphere, whose bottom depth varies also to coincide with the 1300 °C isotherm. Extensional detachments have been identified in the field, but the existence of a major detachment, buried but close to the surface in the core of the Lugo dome is not supported by the models as the cause of its thermal evolution. Rather, substantial crustal thickening is necessary in any case to explain the whole thermal history of the dome.

The main recognized pulses of granite production are explained by the thermal models based only in orogenic crustal thickening followed by thermal relaxation and subsequent lithospheric collapse and extension. The mantle contribution recognized in some groups of Variscan granitoids can be explained by partial melting during extension and thermal re-equilibration. Mantle delamination is not necessary to explain the thermal evolution of the crust at any stage of the orogenic evolution.

Acknowledgements. – This contribution has been funded by the Spanish Government agency Dirección General de Investigación, through project CGL2004-04306-CO2/BTE. J.E. Alcock benefited from a six months position as Visiting Professor in the Universidad de Salamanca, which was essential to the coordination necessary for the development of the thermal models, and is kindly acknowledged. The manuscript has beneficed from reviews by Michel Ballèvre and Olivier Vanderhaeghe, whose scientific suggestions and contribution to the correctness and clarity of the text are kindly acknowledged.

References

Abati J., Arenas R., Martínez Catalán J.R. & Díaz García F. (2003). – Anticlockwise P-T path of granulites from the Monte Castelo Gabbro (Órdenes Complex, NW Spain). – *J. Petrol.*, **44**, 305-327.

Aller J. & Bastida F. (1993). – Anatomy of the Mondoñedo Nappe basal shear zone (NW Spain). – *J. Struct. Geol.*, **15**, 1405-1419.

Ancochea E., Arenas R., Brandle J.L. Peinado, M. & Sagredo J. (1988). – Caracterización de las rocas metavolcánicas silúricas del Noroeste del Macizo Ibérico. – *Geociências, Univ. Aveiro*, **3**, 23-34.

Aranguren A. & Tubía J.M. (1992). – Structural evidence for the relationship between thrusts, extensional faults and granite intrusions in the Variscan belt of Galicia (Spain). – *J. Struct. Geol.*, **14**, 1229-1237.

Arenas R. (1988). – Evolución petrológica y geoquímica de la unidad alóctona inferior del complejo metamórfico básico-ultrabásico de Cabo Ortegal (Unidad de Moeche) y del Silúrico paraautóctono, Cadena Hercínica Ibérica (NW de España): A Coruña, Spain. – *Corpus Geologicum Gallaeciae, Lab. Xeol. Laxe*, **4**, 543 p.

Arenas R. (1991). – Opposite P,T,t paths of Hercynian metamorphism between the upper units of the Cabo Ortegal Complex and their substratum (northwest of the Iberian Massif). – *Tectonophysics*, **191**, 347-364.

Arenas R. & Martínez Catalán J.R. (2003). – Low-P metamorphism following a Barrovian-type evolution. Complex tectonic controls for a common transition, as deduced in the Mondoñedo thrust sheet (NW Iberian Massif). – *Tectonophysics*, **365**, 143-164.

Arenas R., Rubio Pascual F.J., Díaz García F. & Martínez Catalán J.R. (1995). – High-pressure micro-inclusions and development of an inverted metamorphic gradient in the Santiago Schists (Ordenes Complex, NW Iberian Massif, Spain): evidence of subduction and syn-collisional decompression. – *J. Metam. Geol.*, **13**, 141-164.

Arenas R., Abati J., Martínez Catalán J.R., Díaz García F. & Rubio Pascual F.J. (1997). – P-T evolution of eclogites from the Agualada Unit (Ordenes Complex, NW Iberian Massif, Spain): Implications for crustal subduction. – *Lithos*, **40**, 221-242.

Arenas R., Martínez Catalán J.R., Sánchez Martínez S., Díaz García F., Abati J., Fernández-Suárez J., Andonaegui P. & Gómez-Barreiro J. (2007). – Paleozoic ophiolites in the Variscan suture of Galicia (northwest Spain): distribution, characteristics and meaning. *In*: R.D. Hatcher Jr., M.P. Carlson, J.H. McBride & J.R. Martínez Catalán, Eds., 4D framework of continental crust. – *Geol. Soc. Amer. Mem.*, **200**, 425-444.

Ayarza P. & Martínez Catalán J.R. (2007). – Potential field constraints on the deep structure of the Lugo gneiss dome (NW Spain). – *Tectonophysics*, **439**, 67-87.

Ayarza P., Martínez Catalán J.R., Gallart J., Dañobeitia J.J. & Pulgar J.A. (1998). – Estudio sísmico de la corteza ibérica norte 3.3: a seismic image of the Variscan crust in the hinterland of the NW Iberian Massif. – *Tectonics*, **17**, 171-186.

Bastida F. (1981). – Medida de la deformación a partir de pliegues paralelos aplastados. – *Trab. Geol. Univ. Oviedo*, **11**, 15-33.

Bastida F., Martínez Catalán J.R. & Pulgar J.A. (1986). – Structural, metamorphic and magmatic history of the Mondoñedo nappe (Hercynian belt, NW Spain). – *J. Struct. Geol.*, **8**, 415-430.

Bellido Mulas F., González Lodeiro F., Klein E., Martínez Catalán J.R. & Pablo Maciá J.G. de. (1987). – Las rocas graníticas hercínicas del Norte de Galicia y occidente de Asturias. – *Mem. Inst. Geol. Min. España*, **101**, 157 p.

Block L. & Royden L.H. (1990). – Core complex geometries and regional scale flow in the lower crust. – *Tectonics*, **9**, 557-567.

Burg J.-P., Kaus B.J.P. & Podladchikov Y.Y. (2004). – Dome structures in collision orogens: Mechanical investigation of the gravity/compression interplay. *In*: D.L. Whitney, C. Teyssier & C.S. Siddoway, Eds., Gneiss domes in orogeny. – *Geol. Soc. Amer. Sp. Paper*, **380**, 47-66.

Burg J.-P., Van Den Driessche J. & Brun J.-P. (1994). – Syn-to post-thickening extension: mode and consequences. – *C. R. Geoscience*, **319**, 1019-1032.

Capdevila R. (1969). – Le métamorphisme régional progressif et les granites dans le segment hercynien de Galice nord oriental (NW de l'Espagne). – Thèse Sci., Montpellier, 430 p.

Capdevila R. & Floor P. (1970). – Les differents types de granites hercyniens et leur distribution dans le Nord-Ouest de l'Espagne. – *Bol. Geol. Min., Inst. Geol. Min. España*, **81**, 215-225.

Capdevila R. & Vialette Y. (1970). – Estimation radiométrique de l'âge de la deuxième phase tectonique hercynienne en Galice moyenne (Nord-Ouest de l'Espagne). – *C. R. Geoscience*, **270**, 2527-2530.

Chatterjee N.D. & Johannes W. (1974). – Thermal stability and standard thermodynamic properties of synthetic $2M_1$-muscovite ($KAl_2(AlSi_3O_{10}(OH)_2$). – *Contr. Mineral. Petrol.*, **48**, 89-114.

Córdoba D., Banda E. & Ansorge J. (1987). – The Hercynian crust in northwestern Spain: a seismic survey. – *Tectonophysics*, **132**, 321-333.

Dallmeyer R.D., Martínez Catalán J.R., Arenas R., Gil Ibarguchi J.I., Gutiérrez Alonso G., Farias P., Aller J. & Bastida F. (1997). – Diachronous Variscan tectonothermal activity in the NW Iberian Massif: Evidence from $^{40}Ar/^{39}Ar$ dating of regional fabrics. – *Tectonophysics*, **277**, 307-337.

Davy Ph. & Gillet Ph. (1986). – The stacking of thrust slices in collision zones and its thermal consequences. – *Tectonics*, **5**, 913-929.

Díez Montes A. (2007). – La geología del dominio "Ollo de Sapo" en las comarcas de Sanabria y Terra de Bolo. – *Laboratorio Xeolóxico de Laxe, Serie Nova Terra*, **34**, 494 p.

England P.C. & Thompson A.B. (1984). – Pressure-temperature-time paths of regional metamorphism I. Heat transfer during the evolution of regions of thickened continental crust. – *J. Petrol.*, **25**, 894-928.

England P.C. & Thompson A.B. (1986). – Some thermal and tectonic models for crustal melting in continental collision zones. *In*: M.P. Coward & A.C. Ries, Eds., Collision tectonics. – *Geol. Soc. London Sp. Publ.*, **19**, 83-94.

Escuder Viruete J., Arenas R. & Martínez Catalán J.R. (1994). – Tectonothermal evolution associated with Variscan crustal extension in the Tormes Gneiss Dome (NW Salamanca, Iberian Massif, Spain). – *Tectonophysics*, **238**, 117-138.

Escuder Viruete J., Indares A. & Arenas R. (1997). – P-T path determinations in the Tormes Gneissic Dome, NW Iberian Massif, Spain. – *J. Metam. Geol.*, **15**, 645-663.

Escuder Viruete J., Indares A. & Arenas R. (2000). – P-T paths derived from garnet growth zoning in an extensional setting: an example from the Tormes Gneissic Dome (Iberian Massif, Spain). – *J. Petrol.*, **41**, 1488-1518.

Farias P., Gallastegui G., González-Lodeiro F., Marquínez J., Martín Parra L.M., Martínez Catalán J.R., Pablo Maciá J.G. & Rodríguez Fernández L.R. (1987). – Aportaciones al conocimiento de la litoestratigrafía y estructura de Galicia Central. – *Mem. Fac. Ciências, Univ. Porto*, **1**, 411-431.

Fayon A.K., Whitney D.L. & Teyssier C. (2004). – Exhumation of orogenic crust: Diapiric ascent versus low-angle normal faulting. *In*: D.L. Whitney, C. Teyssier & C.S. Siddoway, Eds., Gneiss domes in orogeny. – *Geol. Soc. Amer. Sp. Paper*, **380**, 129-139.

Fernández M., Marzán I., Correia A. & Ramalho E. (1998). – Heat flow, heat production, and lithospheric thermal regime in the Iberian Peninsula. – *Tectonophysics*, **291**, 29-53.

Fernández-Suárez J., Dunning G.R., Jenner G.A. & Gutiérrez-Alonso G. (2000). – Variscan collisional magmatism and deformation in NW Iberia: constraints from U-Pb geochronology of granitoids. – *J. Geol. Soc., London*, **157**, 565-576.

Galán G., Pin C. & Duthou J.-L. (1996). – Sr-Nd isotopic record of multi-stage interactions between mantle-derived magmas and crustal components in a collision context – The ultramafic-granitoid association from Vivero (Hercynian belt, NW Spain). – *Chem. Geol.*, **131**, 67-91.

Gerbi C.C., Johnson S.E. & Koons P.O. (2006). – Controls on low-pressure anatexis. – *J. Metam. Geol.*, **24**, 107-118

Gerya T.V., Perchuk L.L., Maresch W.V. & Willner A.P. (2004). – Inherent gravitational instability of hot continental crust: Implications for doming and diapirism in granulite facies terrains. *In*: D.L. Whitney, C. Teyssier & C.S. Siddoway, Eds., Gneiss domes in orogeny. – *Geol. Soc. Amer. Sp. Paper*, **380**, 97-115.

Gil Ibarguchi J.I. & Arenas R. (1990). – Metamorphic evolution of the allochthonous complexes from the Northwest of the Iberian Peninsula. *In*: R.D. Dallmeyer & E. Martínez García, Eds., Pre-Mesozoic geology of Iberia. – Springer-Verlag, Heidelberg, 237-246.

Hudleston P.J. (1973). – Fold morphology and some geometrical implications of theories of fold development. – *Tectonophysics*, **16**, 1-46.

Iglesias Ponce de León M. & Choukroune P. (1980) – Shear zones in the Iberian arc. – *J. Struct. Geol.*, **2**, 63-68.

Jamieson R.A. (1986). – P-T paths from high temperature shear zones beneath ophiolites. – *J. Metam. Geol.*, **4**, 3-22.

Lancelot J.R., Allegret A. & Iglesias Ponce de León M. (1985). – Outline of Upper Precambrian and Lower Paleozoic evolution of the Iberian Peninsula according to U-Pb dating of zircons. – *Earth Planet. Sci. Letters*, **74**, 325-337.

Le Breton N. & Thompson A.B. (1988). – Fluid-absent (dehydration) melting of biotite in metapelites in the early stages of crustal anatexis. – *Contrib. Mineral. Petrol.*, **99**, 226-237.

Luth W.D., Jahns R.H. & Tuttle O.F. (1964). – The granite system at pressures of 4 to 10 kilobars. – *J. Geophys. Res.*, **69**, 659-773.

Marcos A., Marquínez J., Pérez-Estaún A., Pulgar J.A. & Bastida F. (1984). – Nuevas aportaciones al conocimiento de la evolución tectonometamórfica del Complejo de Cabo Ortegal (NW de España). – *Cuad. Lab. Xeol. Laxe*, **7**, 125-137.

Marcos A., Farias P., Galán G., Fernández F.J. & Llana-Fúnez S. (2002). – Tectonic framework of the Cabo Ortegal Complex: A slab of lower crust exhumed in the Variscan orogen (northwestern Iberian Peninsula). *In*: J.R. Martínez Catalán, R.D. Hatcher, R. Arenas & F. Díaz García, Eds., Variscan-Appalachian dynamics: the building of the Late Paleozoic basement. – *Geol. Soc. Amer. Sp. Paper*, **364**, 125-142.

Martínez F.J., Julivert M., Sebastian A., Arboleya M.L. & Gil Ibarguchi J.I. (1988). – Structural and thermal evolution of the high-grade areas in the northwestern parts of the Iberian Massif. – *Am. J. Science*, **288**, 969-996.

Martínez Catalán J.R. (1985). – Estratigrafía y estructura del domo de Lugo (Sector Oeste de la zona Asturoccidental-leonesa): A Coruña, Spain. – *Corpus Geologicum Gallaeciae, Lab. Xeol. Laxe*, **2**, 291 p.

Martínez Catalán J.R., Arenas R., Díaz García F., Rubio Pascual F.J., Abati J. & Marquínez J. (1996). – Variscan exhumation of a subducted Paleozoic continental margin: The basal units of the Ordenes Complex, Galicia, NW Spain. – *Tectonics*, **15**, 106-121.

Martínez Catalán J.R., Díaz García F., Arenas R., Abati J., Castiñeiras P., González Cuadra P., Gómez Barreiro J. & Rubio Pascual F. (2002). – Thrust and detachment systems in the Ordenes Complex (northwestern Spain): Implications for the Variscan-Appalachian geodynamics. *In*: J.R. Martínez Catalán, R.D. Hatcher, R. Arenas & F. Díaz García, Eds., Variscan-Appalachian dynamics: the building of the Late Paleozoic basement. – *Geol. Soc. Amer. Sp. Paper*, **364**, 163-182.

Martínez Catalán J.R., Arenas R. & Díez Balda M.A. (2003). – Large extensional structures developed during emplacement of a crystalline thrust sheet: the Mondoñedo nappe (NW Spain). – *J. Struct. Geol.*, **25**, 1815-1839.

Martínez Catalán J.R., Arenas R. & Díez Balda M.A. (2004). – Zona Asturoccidental-leonesa: Extensión y metamorfismo de baja presión en el Manto de Mondoñedo. *In*: J.A. Vera, Ed., Geología de España. – Sociedad Geológica de España – Instituto Geológico y Minero de España, Madrid, 58-60.

MARTÍNEZ CATALÁN J.R., ARENAS R., DÍAZ GARCÍA F., GÓMEZ-BARREIRO J., GONZÁLEZ CUADRA P., ABATI J., CASTIÑEIRAS P., FERNÁNDEZ-SUÁREZ J., SÁNCHEZ MARTÍNEZ S., ANDONAEGUI P., GÓNZALEZ CLAVIJO E., DÍEZ MONTES A., RUBIO PASCUAL F.J. & VALLE AGUADO B. (2007). – Space and time in the tectonic evolution of the northwestern Iberian Massif. Implications for the Variscan belt. *In*: R.D. HATCHER JR., M.P. CARLSON, J.H. MCBRIDE & J.R. MARTÍNEZ CATALÁN, Eds., 4D framework of continental crust. – *Geol. Soc. Amer. Mem.*, **200**, 403-423.

MATTE PH. (1968). – La structure de la virgation hercynienne de Galice (Espagne). – *Rev. Géol. Alpine*, **44**, 1-128.

MCKENZIE D.P. & BICKLE M.J. (1988). – The volume and composition of melt generated by extension of the lithosphere. – *J. Petrol.*, **29**, 625-679.

MEANS W.D. (1976). – Stress and strain. – Springer Verlag, Berlin, 339 p.

MONTERO P., BEA F., GONZÁLEZ LODEIRO F., TALAVERA C. & WHITEHOUSE M.J. (2007). – Zircon ages of the metavolcanic rocks and metagranites of the Ollo de Sapo domain in central Spain: implications for the Neoproterozoic to Early Palaeozoic evolution of Iberia. – *Geol. Mag.*, **144**, 963-976.

ORTEGA L.A., ARANGUREN A., MENÉNDEZ M. & GIL IBARGUCHI I. (2000). – Petrogénesis, edad y emplazamiento del granito tardi-hercínico de Veiga (antiforme del Ollo de Sapo, Noroeste de España). – *Cuad. Lab. Xeol. Laxe*, **25**, 265-268.

PARSONS B. & MCKENZIE D. (1978). – Mantle convection and the thermal structure of the plates. – *J. Geophys. Res.*, **83**, 4485-4496.

PEACOCK S.M. (1989). – Thermal modeling of metamorphic-pressure-temperature-time paths. *In*: SPEAR F.S. & PEACOCK S.M., Eds., Metamorphic pressure-temperature-time paths. – *Am. Geophys. Union, Short Course in Geology*, **7**, 57-102.

PEACOCK S.M. (1990). – Numerical simulation of metamorphic pressure-temperature-time paths and fluid production in subducting slabs. – *Tectonics*, **9**, 1197-1211.

PEACOCK S.M. (1991). – Numerical simulation of subduction zone pressure-temperature-time paths: constraints on fluid production and arc magmatism. – *Phil. Trans. Roy. Soc., London*, **A335**, 341-353.

POWELL R. & HOLLAND T. (1990). – Calculated mineral equilibria in the pelite system, KFMASH (K_2O-FeO-MgO-Al_2O_3-SiO_2-H_2O). – *Am. Miner.*, **75**, 367-380.

RAMSAY J.G. (1967). – Folding and fracturing of rocks. – McGraw-Hill, New York, 568 p.

RAMSAY J.G. & HUBER M.I. (1987). – The techniques of modern structural geology. Vol. 2: Folds and fractures. – Academic Press, London, 309-700.

RAPP R.P. & WATSON E.B. (1995). – Dehydration melting of metabasal at 8-32 kbar; implications for continental growth and crust-mantle recycling. – *J. Petrology*, **36**, 891-931.

RECHE J., MARTÍNEZ F.J., ARBOLEYA M.L., DIETSCH C. & BRIGGS W.D. (1998). – Evolution of a kyanite-bearing belt within a HT-LP orogen: the case of NW Variscan Iberia. – *J. Metam. Geol.*, **16**, 379-394.

REGÊNCIO MACEDO C.A. (1988). – Granitóides, complexo xisto-grauváquico e Ordovícico na região entre Trancoso e Pinhel (Portugal Central). – Thèse Sci., Coimbra, 430 p.

RIES A.C. (1979). – Variscan metamorphism and K-Ar dates in the Variscan fold belt of S Brittany and NW Spain. – *J. Geol. Soc., London*, **136**, 89-103.

ROMÁN-BERDIEL T., PUEYO-MORER E.L. & CASAS-SÁIZ A.M. (1995). – Granite emplacement during contemporary shortening and normal faulting: structural and magnetic study of the Veiga Massif (NW Spain). – *J. Struct. Geol.*, **17**, 1689-1706.

SPEAR F.S. (1989). – Petrologic determinations of metamorphic pressure-temperature-time paths. *In*: F.S. SPEAR & S.M. PEACOCK, Eds., Metamorphic pressure-temperature-time paths. – *Am. Geophys. Union, Short Course in Geology*, **7**, 1-55.

SPEAR F.S., KOHN J.M. & CHENEY J.T. (1999). – P-T paths from anatectic pelites. – *Contrib. Mineral. Petrol.*, **134**, 17-32.

STÜWE K. (2002). – Geodynamics of the lithosphere. – Springer-Verlag, Berlin, 449 p.

THOMPSON A.B. (2001). – P-T paths, H_2O recycling, and depth of crystallization for crustal melts: Physics and chemistry of the Earth, Part A. – *Solid Earth and Geodesy*, **26**, 231-237.

THOMPSON A.B. & ENGLAND P.C. (1984). – Pressure-temperature-time paths of regional metamorphism II. Their inference and interpretation using mineral assemblages in metamorphic rocks. – *J. Petrology*, **25**, 929-955.

THOMPSON A.B. & RIDLEY J.R. (1987). – Pressure-temperature-time (P-T-t) histories of orogenic belts. – *Phil. Trans. Roy. Soc., London*, **A321**, 27-45.

TIREL C., BRUN J.-P. & BUROV E. (2004). – Thermomechanical modeling of extensional gneiss domes. *In*: D.L. WHITNEY, C. TEYSSIER & C.S. SIDDOWAY, Eds., Gneiss domes in orogeny. – *Geol. Soc. Amer. Sp. Paper*, **380**, 67-78.

TURCOTTE D.L. & SCHUBERT G. (1982). – Geodynamics. Applications of continuum physics to geological problems. – John Wiley & Sons, New York, 450 p.

VACAS PEÑA J.M. (2001). – Isogons: a program in pascal to draw the dip isogons of folds. – *Comp. & Geosci.*, **27**, 601-606.

VALLE AGUADO B., AZEVEDO M.R., SCHALTEGGER U., MARTÍNEZ CATALÁN J.R. & NOLAN J. (2005). – U-Pb zircon and monazite geochronology of Variscan magmatism related to syn-convergence extension in Central northern Portugal. – *Lithos*, **82**, 169-184.

VALVERDE-VAQUERO P. & DUNNING G.R. (2000). – New U-Pb ages for Early Ordovician magmatism in Central Spain. – *J. Geol. Soc., London*, **157**, 15-26.

VEGAS N., ARANGUREN A. & TUBÍA J.M. (2001). – Granites built by sheeting in a fault stepover (the Sanabria Massifs, Variscan Orogen, NW Spain). – *Terra Nova*, **13**, 180-187.

WHITNEY D.L., TEYSSIER C. & VANDERHAEGHE O. (2004). – Gneiss domes and crustal flow. *In*: D.L. WHITNEY, C. TEYSSIER & C.S. SIDDOWAY Eds., Gneiss domes in orogeny. – *Geol. Soc. Amer. Sp. Paper*, **380**, 15-33.